

1 Responses to Reviewer 1

2
3 We thank the reviewer for the constructive comments and suggestions which will be very helpful as we revise the
4 manuscript. Below the complete reviewer comments are shown along with detailed responses to each comment
5 (reviewer comments in black, responses in blue font)

6 7 Review:

8
9 Dear Editor, I read with great interest this manuscript related to the application of an optimization procedure
10 combining satellite and BGC-Argo floats measurements with a biogeochemical model of the Gulf of Mexico. The
11 manuscript is well organized and provides important insight to improve model parameterizations combining state-
12 of-the-art sensors data-streams. I found particularly important the results showing the importance of combining
13 chlorophyll and bbp measured by BGCArgo to optimize the model in terms of POC and export. In my opinion it
14 is also important the results that, to a large extent, the optimization procedure carried out on the 1D model can be
15 translated to the 3D model implementation. Therefore, I suggest the publication of this manuscript after minor
16 revisions reported below. My comments are indented in blue.

17
18 Minor revisions

19
20 **Response:** We would like to thank the reviewer for the positive assessment and constructive comments.

21 22 1. Introduction

23 Pg2 line 45. because the number of parameters increases exponentially with the number of state variables (Denman,
24 2003).

25 I would expect a polynomial [quadratic] not an exponential increase of the parameter number vs state variable
26 number. In fact, Denman (2003) provides a polynomial formula for the increase of fluxes vs state variables and
27 elaborates the estimate of increase of parameters basing on this formula.

28 **Response:** Thanks for noting this. As suggested by Reviewer #2, we removed this paragraph in our revised
29 manuscript.

30
31 Pg3 lines 68-70. This is especially problematic in oligotrophic regions where the maximum chlorophyll
32 concentration (referred as the deep chlorophyll maximum, DCM) is pronounced near the base of the euphotic zone
33 because of photo-acclimation (Cullen, 2015; Fennel and Boss, 2003).

34 Could Authors explain better what they mean? In general DCM can appear in mathematical terms even without
35 photo-acclimation (e.g. Varela et al. 1994, Ryabov and Blasius 2008). I suggest Authors to be more specific on this
36 point. Nonetheless, the effect of photo-acclimation mentioned here could produce an enhancement of the DCM
37 feature [already explainable by mechanisms other than photo-acclimation] and could be particularly important for
38 the specific area of the GoM.

39 References

40 Varela, R. A., A. Cruzado, and Joaquín Tintoré. "A simulation analysis of various biological and physical factors
41 influencing the deep-chlorophyll maximum structure in oligotrophic areas." *Journal of Marine Systems* 5.2 (1994):
42 143-157.

43 Ryabov, Alexei B., and Bernd Blasius. "Population growth and persistence in a heterogeneous environment: the
44 role of diffusion and advection." *Mathematical Modelling of Natural Phenomena* 3.3 (2008): 42-86.

45 **Response:** Here we are referring to the fact that in oligotrophic regions where the deep chlorophyll maximum is
46 pronounced and located relatively deep in the water column, satellite data of surface chlorophyll are insufficient
47 for characterizing the vertically inhomogeneous chlorophyll structure.

48 Furthermore, in general in the ocean, DCMs are maxima in chlorophyll but not biomass. Typically, there is no
49 biomass maximum associated with the DCM, it is merely an artifact of photoacclimation acting on the
50 exponentially declining light field. This is especially obvious in oligotrophic regions. While it might be true that a
51 biomass maximum coincident with the DCM can be created in mathematical equations as the reviewer suggests
52 (e.g. this is true in an NPDZ model that does not account for photoacclimation), this does not accurately reflect
53 reality.

54 In our revised manuscript, we changed this sentence into:

55 *"This is especially problematic in oligotrophic regions where the deep chlorophyll maximum (DCM) is relatively*
56 *deep and hardly observed by the satellite (Cullen, 2015; Fennel and Boss, 2003)."*

57 We also add some brief comments of DCM and biomass maximum (P12 Lines 299-301) when the first time we
58 talked about DCM in our model results to make these two points clearer.

59

60 **2. Study Region**

61 I would suggest Authors to add information about the recirculation times of the GoM waters with respect to the
62 Atlantic Ocean boundary conditions (BC), this would give an idea on the relevance of the BC in the experiments.

63 **Response:** The recirculation times of the open Gulf is relatively long (certainly much longer than our simulation),
64 but we are not aware of a study that specifically looks at this question. We feel that a discussion of recirculation
65 times is well outside of the intended scope of our manuscript. Our treatment of the boundary conditions is consistent
66 with previous modeling studies with the same or a slightly modified version of the same model (Xue et al. 2013,
67 2016, Yu et al. 2019), hence we are reasonably confident in our set-up.

68 Xue, Z., He, R., Fennel, K., Cai, W.-J., Lohrenz, S., Huang, W.-J., Tian, H., Ren, W., and Zang, Z.: Modeling pCO₂
69 variability in the Gulf of Mexico, *Biogeosciences*, 13, 4359-4377. 2016.

70 Xue, Z., He, R., Fennel, K., Cai, W.-J., Lohrenz, S., and Hopkinson, C., Modeling ocean circulation and
71 biogeochemical variability in the Gulf of Mexico, *Biogeosciences*, 10, 7219-7234, doi:10.5194/bg-10-7219-2013.
72 2013.

73 Yu, L., Fennel, K., Wang, B., Laurent, A., Thompson, K. R., and Shay, L. K.: Evaluation of nonidentical versus
74 identical twin approaches for observation impact assessments: an ensemble-Kalman-filter-based ocean assimilation
75 application for the Gulf of Mexico, *Ocean Science*, 15, 1801–1814, <https://doi.org/10.5194/os-15-1801-2019>, 2019

76

77 Moreover it would be interesting to know what are the observed dominant plankton species, or plankton functional
78 types, in the open-ocean part of GoM [pico-phytoplankton and flagellates?]. This could be useful to figure out the
79 implications of the choice of considering one phytoplankton in the model when compared to data.

80 **Response:** We chose a one-phytoplankton model because it is simple and thus more likely that the model
81 parameters can be constrained by the limited observations available. If we were using a more complex model, there

82 would be more uncertain parameters making model optimization much more difficult. In addition, this relatively
83 simple model has been successfully used to study the biogeochemical variabilities (Xue et al., 2013) and CO₂ air-
84 sea fluxes (Xue et al., 2016) in the Gulf of Mexico. The same model has also been used for a number of studies of
85 hypoxia generation in the northern Gulf of Mexico (e.g. Fennel et al. 2011, Yu et al. 2015, Laurent et al. 2017,
86 2018, Große et al. 2019). While we agree with the reviewer that analyses of model complexity are important and
87 interesting, such a discussion is outside of the intended scope of this manuscript. There are dedicated publications
88 on this (e.g. Kuhn et al. 2019). We believe we are making a novel contribution on a different important topic in
89 this manuscript.

90

91 Fennel, K., Hetland, R., Feng, Y., and DiMarco, S.: A coupled physical-biological model of the Northern Gulf of
92 Mexico shelf: model description, validation and analysis of phytoplankton variability, *Biogeosciences*, 8, 1881–
93 1899, <https://doi.org/10.5194/bg-8-1881-2011>, 2011.

94 Große, F., Fennel, K., & Laurent, A.: Quantifying the relative importance of riverine and open-ocean nitrogen
95 sources for hypoxia formation in the northern Gulf of Mexico. *Journal of Geophysical Research: Oceans*, 124.
96 <https://doi.org/10.1029/2019JC015230>. 2019.

97 Kuhn, A. Fennel, K.: Evaluating ecosystem model complexity for the northwest North Atlantic through surrogate-
98 based optimization, *Ocean Modelling*, <https://doi.org/10.1016/j.ocemod.2019.101437>, 2019.

99 Laurent, A., K. Fennel, W.-J. Cai, W.-J. Huang, L. Barbero, and R. Wanninkhof: Eutrophication- induced
00 acidification of coastal waters in the northern Gulf of Mexico: Insights into origin and processes from a coupled
01 physical-biogeochemical model, *Geophys. Res. Lett.*, 44, 946–956, doi:10.1002/2016GL071881. 2017.

02 Laurent, A., Fennel, K., Ko, D. S., & Lehrter, J.: Climate change projected to exacerbate impacts of coastal
03 eutrophication in the northern Gulf of Mexico. *Journal of Geophysical Research: Oceans*, 123, 3408–3426.
04 <https://doi.org/10.1002/2017JC013583>. 2018.

05 Xue, Z., He, R., Fennel, K., Cai, W.-J., Lohrenz, S., and Hopkinson, C.: Modeling ocean circulation and
06 biogeochemical variability in the Gulf of Mexico, *Biogeosciences*, 10, 7219–7234, <https://doi.org/10.5194/bg-10-7219-2013>, 2013.

08

09 Xue, Z., He, R., Fennel, K., Cai, W.-J., Lohrenz, S., Huang, W.-J., Tian, H., Ren, W., and Zang, Z.:
10 Modeling pCO₂ variability in the Gulf of Mexico, *Biogeosciences*, 13, 4359–4377, <https://doi.org/10.5194/bg-13-4359-2016>, 2016.

12

13 Yu, L., Fennel, K., Laurent, A., Murrell, M. C., and Lehrter, J. C.: Numerical analysis of the primary processes
14 controlling oxygen dynamics on the Louisiana shelf, *Biogeosciences*, 12, 2063–2076, <https://doi.org/10.5194/bg-12-2063-2015>, 2015.

16

17

18 **3. Methods**

19 3.1. Biological observations

20 Pg 5 lines 21-22 SeaWiFS (Sea-viewing Wide Field-of-view Sensor), MODIS (Moderate resolution Imaging
21 Spectroradiometer), and MERIS (medium-spectral resolution imaging spectrometer) products.
22 What about VIIRS? Is it included in the database?, please check.

23 **Response:** We checked and confirmed that indeed VIIRS is included in the database. We corrected it in our revised
24 manuscript (P5 Lines 109-112) and thank the reviewer for pointing this out.

25
26 Pg 5 line 26 and particulate backscattering
27 Pg 5 lines 31-32 Satellite estimates were therefore corrected following the regression equation shown in Figure
28 S2a (Figure S1c).
29 Pg 6 lines 45-48 The bbp700 from the floats is weakly correlated with the satellite estimates ($R^2=0.11$) and
30 generally lower by a factor of ~ 0.45 than the satellite estimates (Figure S2b). The bbp700 profiles were therefore
31 multiplied by 2.2 before being converted to bbp470 following the equ. 1.

32
33 In one case Authors consider the BGC-Argo the ground truth (Pg 5 lines 31-32) in the other Authors correct BGC-
34 Argo with respect to satellite data (Pg 6 lines 45-48). The procedure seems a bit circular, could Authors explain
35 better this part?

36 Pg 6 line 44 extent

37 **Response:** Chlorophyll and backscatter, regardless of whether they are obtained by satellite or in-situ sensors, are
38 proxy measurements. That means they have to be converted and calibrated before they can be used. Here the BGC-
39 Argo floats provided measurements of chlorophyll fluorescence and the volume scattering function at a centroid
40 angle of 140° and a wavelength of 700nm ($\beta(140^\circ, 700\text{nm}) \text{ m}^{-1} \text{ sr}^{-1}$), i.e. a measure of backscatter. The conversion
41 from fluorescence into chlorophyll concentration was based on the sensor manufacturer's calibration. The
42 conversion into bbp700 was performed by us following Green et al. (2014) and by cross-calibration against existing
43 relationships with POC and phytoplankton biomass (Martinez-Vicente et al., 2013; Rasse et al., 2017). The
44 resulting concentrations of phytoplankton biomass and POC as well as the ratio of chlorophyll to phytoplankton
45 biomass are reasonable (please see figures 4 and 10).

46
47 We rewrote these paragraphs and included a more in-depth explanation of this process in our revised manuscript
48 (P5-6 Lines 123-151).

49
50 Green, R. E., Bower, A. S. and Lugo-Fernandez, A.: First Autonomous Bio-Optical Profiling Float in the Gulf of
51 Mexico Reveals Dynamic Biogeochemistry in Deep Waters, PLoS ONE, 9(7), 1–9,
52 doi:10.1371/journal.pone.0101658, 2014.

53
54 Martinez-Vicente, V., Dall'Olmo, G., Tarran, G., Boss, E. and Sathyendranath, S.: Optical backscattering is
55 correlated with phytoplankton carbon across the Atlantic Ocean, Geophysical Research Letters, 40, 1154–1158,
56 doi:10.1002/grl.50252, 2013.

57
58 Rasse, R., Dall'Olmo, G., Graff, J., Westberry, T. K., van Dongen-Vogels, V. and Behrenfeld, M. J.: Evaluating
59 Optical Proxies of Particulate Organic Carbon across the Surface Atlantic Ocean, Frontiers in Marine Science,
60 4(November), 1–18, doi:10.3389/fmars.2017.00367, 2017.

61
62
63 3.2. 3D Model description

64 Pg 7 lines 74-75 Medium-Range Weather Forecast ERA-Interim product with a horizontal resolution of 0.125°
65 (ECMWF reanalysis, <https://www.ecmwf.int/en/forecasts/datasets/reanalysisdatasets/era-interim>).

66 The resolution reported in the link above for ERA-Interim is 80 km this does not match with the 0.125° (~12 km)
67 reported in the manuscript, could Authors double check?

68 **Response:** The resolution of ~80 km is the model grid resolution used by the ERA-Interim's atmospheric model
69 and reanalysis system. However, they also provide their dataset for download in higher (e.g. 0.125°) or coarser
70 resolutions (e.g. 3°) which the original data are interpolated onto. We used the higher-resolution data set as stated
71 in the manuscript.

72 3.3. 1D Model description

73 Pg8 line 10-12. The 1D model, which is similar to that used by Lagman et al. (2014) and Kuhn et al. (2015), covers
74 the upper 200 m of the ocean with a vertical resolution of 5 m and is configured at one location in the central Gulf
75 (see Figure 1).
76

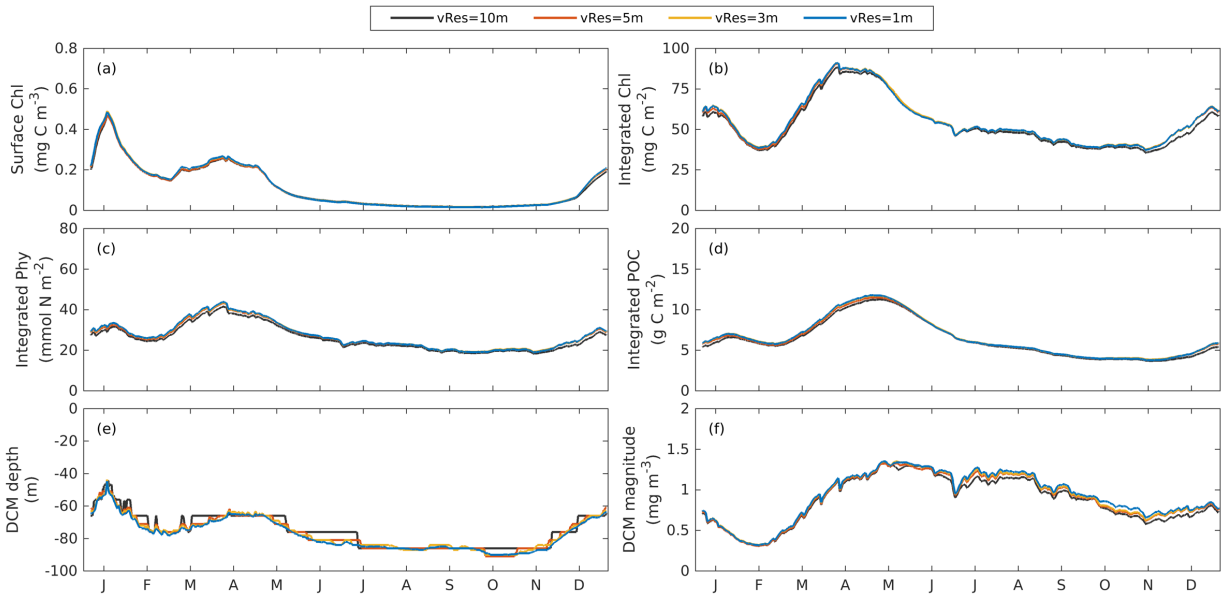
77 Authors should add some comment about the choice of 5 m vertical resolution. What is the 3D model vertical
78 resolution in the same region of the GoM? Why not taking 1m resolution that probably is the vertical resolution of
79 data acquired by BGC-Argo floats?

80 **Response:** There are two main reasons why we chose 5 m. First, the vertical resolution in our BGC-Argo floats is
81 4-6 meters in the upper 200 m. Second, a 5-m vertical resolution in the 1D model keeps the computational cost
82 reasonable. As stated in sections 3.4 and 3.5 of the manuscript, one parameter optimization experiment ran 36,000
83 model simulations (30 simulations/generation * 300 generations*4 replications). It took us about one day to run a
84 single parameter optimization experiment and we performed 13 1D optimization experiments in total (A1-A4, B1-
85 B4, C1-C5). This is in addition to all the 3D model runs we performed.

86 We are confident the vertical resolution is appropriate because we performed sensitivity tests using different
87 vertical resolutions including 10 m, 5 m, 3 m, and 1 m in optimization C4. As shown in Figures 1 and 2 below, the
88 choice of vertical resolution has little impact on model results except for minor jumps in the DCM depth (Figure
89 1e) and DCM magnitude (Figure 2) when a vertical resolution of 10 m is used.

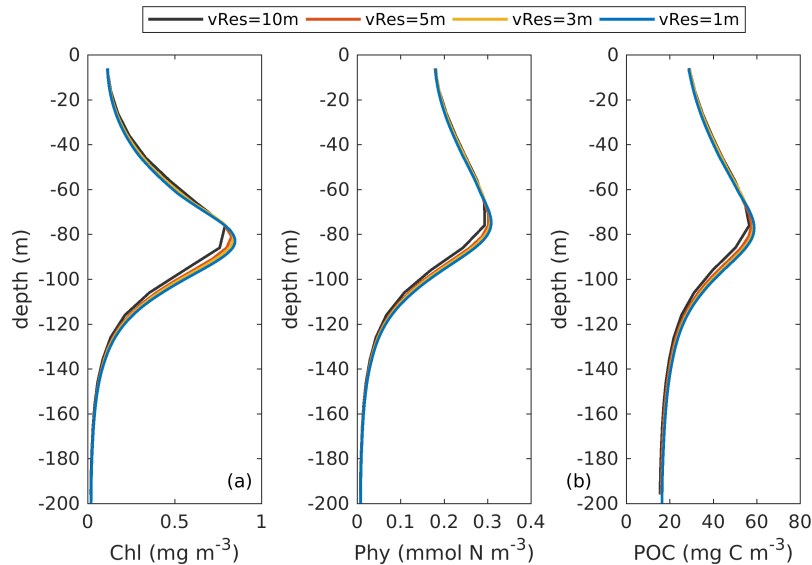
90 The 3D model had 36 terrain-following sigma levels with refined resolution near the surface and bottom layers.
91 The vertical resolution in the 3D model varied from a few meters near the surface to ~50 m near the depth of 200
92 m around the 1D site.

93 In our revised manuscript, we added comments on the 1D model's vertical resolution as suggested (P8 Lines 200-
94 202).
95



96
97
98
99

Figure 1. The simulated annual cycle of surface chlorophyll (a), vertically integrated chlorophyll (b), vertically integrated phytoplankton (c), vertically integrated POC(d), and the depth (e) and magnitude (f) of the DCM by using different vertical resolutions.



00
01
02
03
04
05
06
07

Figure 2. The simulated vertical profiles of chlorophyll, phytoplankton, and POC by using different vertical resolutions.

Pg9 line 13-15. A higher diffusion coefficient ($K_{Z1} = \max(H^2_{MLD}/400, 10)$) is applied in the turbulent surface layer and a lower diffusion coefficient ($K_{Z2} = K_{Z1}/2$) is assigned to the quiescent bottom layer.

What is the unit of measure of $K_{1,2}$, please add this information in the text. If it is m²/s it seems very high, because even with $H_{MLD} = 0 \rightarrow K_{Z1} = 10 \rightarrow K_{Z2} = 5$. Please, add also unit of measure of H_{MLD} , meters?

08 **Response:** The units of K_{Z1} and K_{Z2} are m^2/day . The unit of H_{MLD} is in meters. We added the units as suggested in
09 our revised manuscript (P8 Lines 204-206).

10
11 3.4. Parameter optimization method
12 Pg 11 line 63. and n is the number of base-test pairs including

13 I suggest to use consisting rather than including that in my opinion is confusing. In fact n accounts exactly to what
14 specified (i.e. base –test pairs etc etc)_and not more.

15 **Response:** Revised as suggested.

16
17 The range of variability of W_{phy} spans many orders of magnitude and it is the most sensitive parameter, could
18 Author comment on that?

19 **Response:** The range of sinking speeds for organic matter is large, because pico-plankton sink very slowly, if at
20 all, while large detrital aggregates can sink very fast. We used the same range for all sinking speed in the
21 optimization, as reported in Table 1 (for W_{phy} , W_{SDet} , W_{LDet}), although the speeds for Phy will be in the lower
22 range of the bracket, speeds for $SDet$ in the middle range, and speeds for $LDet$ in the upper range.

23
24 3.5. Parameter optimization experiments
25 Pg 11 line 69-71. For the parameter optimization of the 1D model, satellite chlorophyll within a $3'3$ pixel ($12\text{ km} \times 12$
26 km area) around the 1D station and climatological monthly averages of the profiles from the bio-optical floats were
27 used.

28 Did you considered all the BGC-Argo data available or only the ones near the virtual mooring of your 1D
29 experiment? How you decided the BGC-Argo float to include in the optimization procedure?

30 **Response:** We used all BGC-Argo data by averaging all profiles into climatological monthly bins. We did this
31 because 1) the BGC-Argo profiles were sparsely distributed in the Gulf of Mexico and there were few profiles
32 around the 1D site, and 2) the deep Gulf of Mexico is quite homogenous horizontally.

33 In the revised manuscript, we added statements to make this clearer (P10 Lines 257-259).

34
35 Pg 11 line 81-84. Prior tests have shown that the available observations cannot simultaneously constrain the sinking
36 rates of small and large detritus (w_{SDet} and w_{LDet})Therefore, a constant ratio of 0.1 between these two parameters
37 ($w_{SDet} = 0.1 w_{LDet}$) was imposed and only one of the two was optimized.

38 I suggest Authors to be clearer: I cannot get why the two parameters cannot be constrained. In general, after you
39 completed your optimization procedure you could perturb the parameter 0.1 (ratio between W_{SDet} and W_{LDet}) to
40 see if it corresponds to a minimum for your metrics $F(p)$ or if there are better values other than 0.1. Or the system
41 is unstable if you don't take 0.1? Please explain.

42 **Response:** These two parameters cannot be constrained simultaneously because they can compensate each other:
43 an increase in one parameter can be counteracted by a decrease in the other. This is a well-known and much
44 discussed issue in the parameter optimization literature. Basically, there is no information in the available
45 observations that allows to distinguish between the two. Including both parameters in the optimization will degrade
46 the model's predictive skill. To solve this problem, one can either introduce more independent observations or prior
47 knowledge by, e.g. fixing these parameters to their prior values or defining a link between these parameters.
48 Generally, and also in this case, observations are insufficient to constrain all parameters and prior knowledge about

49 the parameters has to be included. This is the common approach to address the underdetermination problem of
50 parameter optimization in biological models.

51 In this study, the ratio of 0.1 was selected based on the prior values of the two parameters. Perturbing and estimating
52 the ratio between two sinking velocities are equivalent to letting both parameters (wSDet and wLDet) into
53 optimization and may degrade model's predictive skills. Without additional information about the depth
54 distribution of Sdet and Ldet, which is not available, the ratio cannot be constrained.

55 The underdetermination problem and the practice of incorporating prior knowledges is also discussed on P20, L10-
56 28 of our original manuscript.

57
58 Pg 12 line 92 please remove *and* from the equation.

59 **Response:** Revised as suggested.

60 61 **4. Optimization of 1D models**

62 General question: how you define the DCM depth in the presented analyses?

63 **Response:** In this study, the DCM depth was defined as the depth where the subsurface chlorophyll is at its
64 maximum. The definition of DCM depth was included in our revised manuscript (P12 Lines 300-301).

65 66 4.1. Observations and base case

67 Pg 12. Lines 107-109. Unlike the surface chlorophyll, the vertically integrated chlorophyll as well as the
68 phytoplankton and POC over the upper 200 m tend to be more constant with much less seasonality (Figure 3b-d).

69 This statement refers to observation? Please specify. Is it possible to add the error bar to the dots of Figure 3 as in
70 the case of Figure 4?

71 **Response:** Yes, we are referring to observations which are represented by black dots. We clarified this (P12 Line
72 295) in our revised manuscript and added the error bar in Figure 3 as suggested.

73
74 Pg 12 line 14 in June and gradual shoaling after July (Figure 3e), reflecting the seasonality of the solar radiation.

75 With the term reflecting Authors mean that there is direct causality or correlation?

76 **Response:** We think that there is direct causality between the shoaling of DCM depth and solar radiation. In the
77 oligotrophic regions, the DCM is strongly determined by photoacclimation (Cullen, 2015; Fennel and Boss, 2003).
78 Previous studies based on BGC-Argo floats also suggest that the DCM is mainly light driven and located at the
79 level of a particular isolume (e.g. Mignot et al., 2014; Xing et al., 2018). In our case, with the decrease of solar
80 radiation after July, these isolumes and the DCM would therefore become shallower.

81
82 Cullen, J. J.: Subsurface Chlorophyll Maximum Layers : Enduring Enigma or Mystery Solved ?, Annual Review
83 of Marine Science, 7, 207–239, doi:10.1146/annurev-marine-010213-135111, 2015.

84
85 Fennel, K. and Boss, E.: Subsurface maxima of phytoplankton and chlorophyll : Steady-state solutions from a
86 simple model, Limnology and Oceanography, 48(4), 1521–1534, 2003.

87
88 Mignot, A., Claustre, H., Uitz, J., Poteau, A., D'Ortenzio, F. and Xing, X.: Understanding the seasonal dynamics
89 of phytoplankton biomass and the deep chlorophyll maximum in oligotrophic environments: A Bio-Argo float
90 investigation, Global Biogeochemical Cycles, 28(8), 1–21, doi:10.1002/2013GB004781, 2014.

91
92 Xing, X., Qiu, G., Boss, E., & Wang, H. Temporal and vertical variations of particulate and dissolved optical
93 properties in the South China Sea. *Journal of Geophysical Research: Oceans*, 124.
94 <https://doi.org/10.1029/2018JC014880>. 2019.

95
96 Pg 13 line 18 However, it fails to reproduce the deepening of the DCM in June

97 This deepening is related to a physical process (change in some environmental regulating factor) or to a
98 biogeochemical process?

99 **Response:** This deepening is a result of both physical and biological processes. Firstly, as stated in the reply to the
100 last comment, the increase of solar radiation would make the DCM deeper. Secondly, as the water column becomes
101 more stratified in summer, chlorophyll concentrations in the upper layer will be lower as a result of nutrient
102 limitation, which in turn increases light penetration through the water column and thus causing the DCM to deepen.

103
104 4.2. Results of the optimizations

105 4.2.1 Model-data misfits

106 4.2.2 Experiment A

107 Pg 13 line 41-42 The optimal parameter sets (A4, B2, and C4), which are selected based on casespecific misfit
108 from these three groups, will be used in subsequent analyses ...

109 Why Authors decide to use B2 rather than B4 that show a smaller total misfit? Is it better to take a realization with
110 better case-specific misfit or better total misfit?

111 **Response:** Firstly, experiments in group B represent the scenario where we only have chlorophyll observations. In
112 that case, we would have no idea about the model misfit for other variables except chlorophyll or the total misfit.
113 Secondly, the case-specific misfit was the criterion that the parameter optimization procedure used to choose the
114 best half population while “killing” the other half. Hence, using B2 rather than B4 as the optimal parameter sets
115 makes sense.

116 We discussed the choice of B2 in our original manuscript. In realistic parameter optimization applications where
117 only chl and no other observation are available the B2 optimization would be chosen. Revealing this weakness due
118 to insufficient observations can help us to better understand the additional value of BGC-Argo floats and provide
119 some scientific guidance for future parameter optimization studies. This is really the point we are trying to make
120 here.

121
122 4.2.3 Experiment B

123 Pg 14 line 47-49 However, the vertical structure of chlorophyll deteriorates relative to the base case (Figure 4a)
124 because of inappropriate estimates of the initial slope ($\alpha=0.0101$; see table 2) and the maximum ratio of chlorophyll
125 to carbon ($\theta_{\max}=0.0191$; see table 2).

126 If Authors can judge a-priori that the values for α and θ_{\max} resulting from the optimization are not appropriate,
127 why they didn't consider different parameter ranges in the optimization procedure from the beginning, excluding
128 bad values?

129 **Response:** Firstly, we have no prior knowledge of these parameters in the Gulf of Mexico and that is why we run
130 parameter optimization to estimate their values. Our comments on these two parameters here were based on the
131 results of our parameter optimization experiments.

32 Secondly, we feel these two parameters were inappropriate after we compared model results with vertical profiles
33 of chlorophyll and phytoplankton. Since experiment A was designed to represent the scenario where only satellite
34 observations are available, adding the information obtained from the BGC-Argo floats data into experiment A
35 would not be a fair comparison to the other experiments and violate our assumptions of the experiment A.

36
37 Pg 14 lines 57-59. A straightforward interpretation is that the addition of subsurface observations
38 reduces the model's degrees of freedom to fit one single observation type (surface chlorophyll).

39 Does this imply that a model with more parameters (e.g. more phytoplankton species) would fit better?

40 **Response:** Here we mean that the addition of subsurface observations yields more constraints on our biological
41 model because the model should fit both surface and subsurface observations simultaneously.

42 With respect to reviewer's comment, it tends to be true but not always. However, the better fit is often the result of
43 overfitting rather than a true improvement in predictive skill. It is of utmost importance to avoid overfitting. The
44 increased number of parameters in more complex models may increase the risk of degrading model's predictive
45 skills.

46
47 Pg15 line 70 In contrast to the observations where detritus dominates POC ...

48 What observation? Please add reference.

49 **Response:** Here we referred to our BGC-Argo floats shown in Figure 4. We included reference (P14 Lines 354-
50 356) in our revised manuscript as suggested. And as suggested by the Reviewer #3, we changed this sentence into:

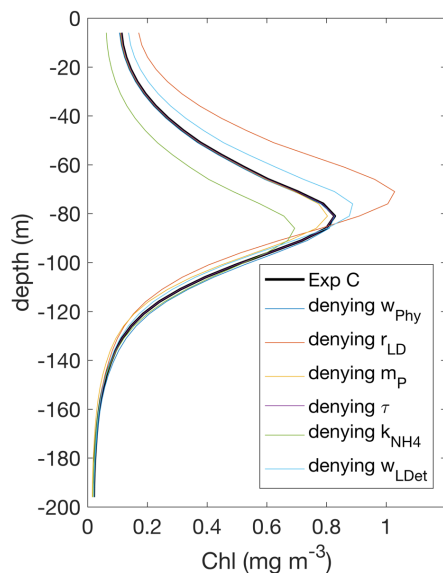
51
52 *“In contrast to the observations where the phytoplankton's contribution is neglectable (Figure 4), the simulated*
53 *POC at 200 m is dominated by phytoplankton (49%)”*

54
55 4.2.4 Experiment C

56 Pg 15 lines 76-78 As shown in Figure 4a, the annually averaged depth of DCM of 80 m coincides with the observed
57 DCM, primarily because experiment reproduces the deepening of the DCM in summer.

58 Interesting. Can Authors explain if there is a specific parameter/mechanism that controls this dynamical deepening
59 of the DCM? Or it is a complex combination of parameters values generating this emergent property?

60 **Response:** As we mentioned above, the deepening of the DCM in the summer resulted from a combination of
61 increased solar radiation and decreased light attenuation in the upper layer. Since the different experiments here
62 used the same inputs of solar radiation, the deepening of the DCM in experiment C must be a result of changes in
63 parameter values which can influence chlorophyll concentrations and hence light attenuation in the upper layer. To
64 illustrate this, we performed sensitivity simulations where we used the optimal parameters from experiment C but
65 set each optimized parameter, one at a time, to its prior value. As shown in Figure 3, the optimization induced
66 changes in large detritus remineralization rate (r_{LD}), half-saturation for NH_4 uptake (K_{NH_4}), and large detritus
67 sinking velocity (w_{LDet}) can have large impacts on chlorophyll concentrations and the depth of DCM.



68
69 Figure 3: Vertical distributions of simulated chlorophyll from different sensitivity tests.

70
71 5. 3D biogeochemical model

72 Could Author explain better the manual correction described at pg 17 lines 24-25? If they consider the corrected
73 values more realistic why they didn't narrowed the parameter variability range in the optimization experiment? Or
74 the 1D vs 3D implementations do not allow this?

75 For example, is there a simple explanation for the need to set KNH4 to 0.01 in the 3D experiments? It would be
76 useful for readers interested in applying this methodology in other areas.

77 **Response:** We did manual modifications because when the resulting parameters were directly applied, the model-
78 data agreement in 3D models was not as well as in 1D models in some respects, but the most important features
79 were well preserved. In experiment C, chlorophyll concentrations in the upper layer of 3D model were lower than
80 the 1D model and farther away from observations. This might be a result of differences between 1D and 3D models
81 and has been also reported in other studies (e.g. Kane et al., 2011; Hoshiba et al., 2018). However, the depth of the
82 DCM and the non-zero POC concentrations at 200 m with appropriate contributions from each component were
83 well preserved. We therefore did some tests manually by tuning one or two parameters and final set the KNH4
84 to 0.01 in order to have a better agreement with respect to observations. All of these modifications were based on
85 our tests.

86 In our case, although the 1D parameter sets could not be used in 3D models directly, they were sufficient to
87 reproduce the main features as in 1D models and largely simplified the following subjective tuning of 3D models
88 by limiting the number of parameters to be adjusted.

89 We included more explanations for the manual modifications (P16 Lines 400-411) and discussion (P20-21 Lines
90 522-530) in our revised manuscript.

91
92 Kane, A., Moulin, C., Thiria, S., Bopp, L., Berrada, M., Tagliabue, A., Crépon, M., Aumont, O. and Badran, F.:
93 Improving the parameters of a global ocean biogeochemical model via variational assimilation of in situ data at

94 five time series stations, Journal of Geophysical Research: Oceans, 116, 1–14, doi:10.1029/2009JC006005, 2011.
95
96 Hoshiba, Y., Hirata, T., Shigemitsu, M., Nakano, H., Hashioka, T., Masuda, Y. and Yamanaka, Y.: Biological data
97 assimilation for parameter estimation of a phytoplankton functional type model for the western North Pacific,
98 Ocean Science, 14, 371–386, doi:10.5194/os-14-371-2018, 2018.
99

00
01 It would be useful to know how the PP from the model is computed: integrating down till the bottom, considering
02 the MLD?

03 **Response:** The primary production in the 3D models was integrated down to 200 m, consistent with the primary
04 production obtained from the 1D models. There is not enough available light below 200 m for photosynthesis to
05 occur, therefore cutting off at 200 m yields the same values of integrated primary production as integration down
06 to the seafloor would. As suggested, we stated this in our revised manuscript (P17 Lines 445).
07

08 6. Discussion

09 6.1 Trade-offs between different observations for parameter optimization

10 In this section Authors use a number of times the following terms poorly constrained, weakly constrained and
11 unconstrained, un-optimized fields, not optimized but well defined. Some definitions can be grasped from section
12 3.5. In my opinion it would make things more simple to have the formal definition of these terms and to know if,
13 in some cases, they are equivalent/synonym.

14 **Response:** The poorly constrained and weakly constrained parameters are synonymous, meaning that they cannot
15 be constrained in confidence. In our study, it can be simply understood that their estimates were inappropriate. The
16 unconstrained and un-optimized fields are equivalent meaning that they were not included in the parameter
17 optimization procedure. The not-optimized but well-defined parameters are those parameters which were not
18 included in the parameter optimization but their prior values were coincidentally reasonable. As suggested, we tried
19 to simplify the language and included these definitions in our revised manuscript.
20

21 Pg 21 lines 36-42 Although this cross-validation at different times and locations may give some indication of
22 overfitting, it cannot determine whether the model reproduces observation through wrong mechanisms because a
23 small misfit of cross-validation can be caused by missing validations of key variables or fluxes, e.g. ignorance of
24 phytoplankton and PP in the experiment B, while a large misfit can be a result of the intrinsic heterogeneity of
25 biological parameters in different times (Mattern et al., 2012) and locations (Kidston et al., 2011), e.g.
26 underestimation of coastal surface chlorophyll in the experiment C.

27 In my opinion the sentence above is not very easy to follow, could Authors simplify?

28 **Response:** As suggested, we revised these sentences into:

29 *“However, even when cross-validation at different times and locations produces large misfits, we cannot conclude*
30 *that the models reproduce observations through wrong mechanisms. This is because the large misfit can be a result*
31 *of intrinsic heterogeneity of biological parameters at different times (Mattern et al., 2012) and locations (Kidston*
32 *et al., 2011).”*
33

34 Pg21 lines 54-55 On the other hand, counter examples exist where the 3D simulations outperform the 1D model
35 (Hoshiba et al., 2018).

36 Could Authors explain better this sentence? Outperform with respect to what aspect?

37 **Response:** Here we mean that applying parameters obtained from 1D models could result in worse or better fitness
38 in 3D models. For instance, Hoshiba et al. 2018 performed parameter optimization by 1D models and applied the
39 resulting parameters in 3D models. As a result, the 3D model had better fitness than the 1D model with respect to
40 vertical profiles of phytoplankton and nitrate (please see their section 3.4 and Figure 10a,b). As suggested, we
41 clarified this in our revised manuscript (P20 Lines 525-526).
42

43 Hoshiba, Y., Hirata, T., Shigemitsu, M., Nakano, H., Hashioka, T., Masuda, Y. and Yamanaka, Y.: Biological data
44 assimilation for parameter estimation of a phytoplankton functional type model for the western North Pacific,
45 Ocean Science, 14, 371–386, doi:10.5194/os-14-371-2018, 2018.

46

47

48

49

50

51

52

53

54

55

56

57

58

59

60

61

62

63

64

65

66

67

68

69

70

71

72

73

74

75

76

77

78

79

80 **Response to Peter Strutton (Referee #2)**

81

82 We thank the reviewer for the constructive comments and suggestions which will be very helpful as we revise the
83 manuscript. Below the complete reviewer comments are shown along with detailed responses to each comment
84 (reviewer comments in black, responses in blue font)

85

86 **Review:**

87

88 This is a very useful contribution that explains the benefit that models can derive from the incorporation of satellite
89 and BGC-Argo observations. The paper is timely and clearly written. I recommend publication after minor
90 revisions.

91

92 **Response:** We would like to thank the reviewer for the positive assessment and constructive comments.

93

94 **Specific comments:**

95 The introduction is comprehensive. It could be shortened a bit (the 3rd and 5th paragraphs could mostly be
96 removed) but this is not essential.

97 **Response:** Thanks for these suggestions. The 5th paragraph is to show weakness of satellite observations which
98 served as the motivation of this study and is highly related to some main conclusions. We would therefore like to
99 keep it in our revised manuscript. As suggested, the 3rd paragraph was removed.

00

01 Methods switch between present and past tense. Also not a big deal, just disconcerting for the reader.

02 **Response:** We looked through the whole Methods section and made the tense appropriate in our revised
03 manuscript.

04

05 P6 L48: Here and in subsequent equations/text I'm a bit confused. The float and satellite measure bbp700 and
06 bbp670 respectively. So why are we now talking about bbp470? And what is meant by 'validated bbp470'?

07 **Response:** We talked about bbp470 because the empirical relationship that we used to estimate phytoplankton and
08 POC was based on bbp470 (please see equ. 2-3). We had to convert measurements of bbp700 and bbp670 to bbp470
09 based on the equ. 1 before we estimated phytoplankton and POC.

10 We rewrote the paragraphs about processing the backscatter and made it clearer in our revised manuscript (P5-6
11 Lines 123-151).

12

13 P6 Eq 2 and 3: What are the units of the terms on the LHS? Please be more specific about what 'Phytoplankton'
14 is. I think it's phytoplankton N.

15 **Response:** Yes, the phytoplankton and POC were in unit of mmol N m^{-3} . We actually have mentioned it in P6-7
16 L58-60 in our original manuscript. We also revised and made it clearer here as suggested (P5 Lines 125-127).

17

18 P11 L69: Here and in section 3.1, the temporal resolution of the satellite data is not specified. I also think a bit
19 more information here would be useful. How are monthly climatologies of the float profiles created? What distance
20 from the 1D site is considered? Maybe this is described elsewhere and I missed it, but I see the other reviewer
21 asked something similar.

22 **Response:** In this study, we used monthly satellite estimates of surface chlorophyll in the parameter optimization.
23 The monthly climatology of float profiles was created by averaging all profiles collected in the Gulf of Mexico into
24 monthly bins. We did this because 1) the BGC-Argo float profiles were sparsely distributed in the Gulf of Mexico
25 and there were insufficient profiles around the 1D site (please see figure 1 in our original manuscript), and 2) the
26 deep ocean part of the Gulf of Mexico is quite homogenous horizontally. As suggested, we included some more
27 description and explanation in our revised manuscript (P5 Line 107 and P10 Lines 256-259).
28

29 P14-15: In the sub-section headings, it wouldn't hurt to remind us what experiments A, B and C are. That is
30 'satellite only' etc.

31 **Response:** Agree. Revised as suggested

32
33 Figures 3 and 8: Why not just put the parameter labels on the y axes?

34 **Response:** Yes, revised as suggested.

35
36 For the 3D case, I think it's correct to say that Figure 8 is an average of all model grid cells where the water depth
37 is >1000m. That's a pretty big area. Yes, it's reasonably uniformly low chlorophyll, so one could make the case
38 that this encompasses a contiguous bio-region. But why not choose a smaller box in the middle of the deep part of
39 the basin, and perhaps one from the shelf, to illustrate the model performance? I suspect the latter will not perform
40 as well, but that would still be interesting to know.

41 **Response:** To the first point, since the BGC-Argo float profiles are sparsely distributed in the deep part of the Gulf
42 of Mexico (please see Figure 1 in our original manuscript), choosing a smaller box would mean that much fewer
43 float profiles are available for the model-data comparison. Also, since the region is quite homogenous horizontally,
44 we feel it is appropriate to average over all. In Figure 4, we show the interquartile range of the profiles in space
45 and time (black bars). These are very similar if calculated only for July. Thus, the error bars in Figure 4 give a good
46 indication of the spatial variability. We added some comments about this in the revised manuscript (P17 Lines 425-
47 427).

48 To the second point, the BGC-Argo floats were deployed only in the deep part of the Gulf, hence no float profiles
49 are available on the shelf. However, we agree that it would be interesting to show the validation in smaller boxes
50 from the deep ocean and shelf, and we included this comparison with satellite surface chlorophyll in the
51 supplementary of our revised manuscript.

52
53 The results proceed in a logical fashion through the different experiments, 1D and 3D. The presentation of the
54 results is clear and concise.

55 **Response:** Thank you, we really appreciate this comment.

56
57 In a paper like this, readers will likely be looking for a clear recommendation: Which of the three options should
58 they choose? I think the conclusions do a good job of summarizing the recommendations and the figures represent
59 what's lost if it's not possible to implement the best case scenario.

60 **Response:** Thank you, we are happy to hear this.

61
62
63

64 Responses to Mara Freilich (Reviewer 3)

65

66 We thank the reviewer for the constructive comments and suggestions which will be very helpful as we revise the
67 manuscript. Below the complete reviewer comments are shown along with detailed responses to each comment
68 (reviewer comments in black, responses in blue font)

69

70 Review:

71

72 This manuscript presents a very well developed and well described parameter optimization process for
73 biogeochemical models using available sea surface and profile observations. The authors show that a model
74 parameterized with both surface chlorophyll from satellite and BGC-Argo profiles of chlorophyll and POC best
75 represents the available observations of ecosystem state and fluxes. The authors demonstrate that the parameter
76 choice has important implications for carbon cycling and export.

77

78 Comments:

79 2. Study Region

80 This section is very useful as an orientation to the region. Since one of the major objectives of the study is to
81 analyze carbon export, it would be useful to include more in this section about what is known about carbon export
82 in the Gulf of Mexico.

83 **Response:** We would like to note that the major objective of this study is to evaluate the trade-offs between
84 different observation types for biological model validation and parameter optimization. Our model-data
85 comparison of carbon export is to illustrate the model performance and additional value brought by BGC-Argo
86 profiles to parameter optimization. Studying the carbon export in the Gulf of Mexico is not within the intended
87 scope of this study.

88

89 3. Methods

90 p. 6, Line 147: Earlier in this section, the satellite chlorophyll was adjusted to the float chlorophyll, but here the
91 float backscattering is adjusted to the satellite backscattering. Why is this? These adjustments may have important
92 implications for the POC profiles and partitioning of POC between phytoplankton, zooplankton, and POC. The
93 reasoning for and implications of this choice should be explained.

94 **Response:** Chlorophyll and backscatter, regardless of whether they are obtained by satellite or in-situ sensors, are
95 proxy measurements. That means they have to be converted and calibrated before they can be used. Here the BGC-
96 Argo floats provided measurements of chlorophyll fluorescence and the volume scattering function at a centroid
97 angle of 140° and a wavelength of 700nm ($\beta(140^\circ, 700\text{nm}) \text{ m}^{-1} \text{ sr}^{-1}$), i.e. a measure of backscatter. The
98 conversion from fluorescence into chlorophyll concentration was based on the sensor manufacturer's calibration.
99 The conversion into $\text{bbp}700$ was performed by us following Green et al. (2014) and by cross-calibration against
00 existing relationships with POC and phytoplankton biomass (Martinez-Vicente et al., 2013; Rasse et al., 2017).
01 The resulting concentrations of phytoplankton biomass and POC as well as the ratio of chlorophyll to
02 phytoplankton biomass are reasonable (please see figures 4 and 10).

03

04 We rewrote these paragraphs and included a more in-depth explanation of this process in our revised manuscript
05 (P5-6 Lines 123-151).

06

07 Since this comment is similar to comments by Reviewer #1 under 3.1, we point also to those responses.

08

09 Green, R. E., Bower, A. S. and Lugo-Fernandez, A.: First Autonomous Bio-Optical Profiling Float in the Gulf of
10 Mexico Reveals Dynamic Biogeochemistry in Deep Waters, PLoS ONE, 9(7), 1–9,
11 doi:10.1371/journal.pone.0101658, 2014.

12

13 Martinez-Vicente, V., Dall’Olmo, G., Tarran, G., Boss, E. and Sathyendranath, S.: Optical backscattering is
14 correlated with phytoplankton carbon across the Atlantic Ocean, Geophysical Research Letters, 40, 1154–1158,
15 doi:10.1002/grl.50252, 2013.

16

17 Rasse, R., Dall’Olmo, G., Graff, J., Westberry, T. K., van Dongen-Vogels, V. and Behrenfeld, M. J.: Evaluating
18 Optical Proxies of Particulate Organic Carbon across the Surface Atlantic Ocean, Frontiers in Marine Science,
19 4(November), 1–18, doi:10.3389/fmars.2017.00367, 2017.

20

21 p. 7, Line 167: What is the range of the vertical resolution of the ROMS model in the upper 200 meters? This
22 information will be useful for comparison with the 1D model.

23 **Response:** The 3D model had 36 terrain-following sigma levels which means that the vertical resolution varies
24 with the bathymetry. The vertical resolution in the 3D model ranges from a few meters near the surface to ~50 m
25 near the depth of 200 m around the 1D site. In the revised manuscript, we added a simple description of 3D model
26 resolution to be compared with the 1D model resolution (P8 Lines 200-202).

27

28 We also point to our response to comments by Reviewer #1 under 3.2.

29

30 p. 8, Line 187: Since the biogeochemical model functional forms are essential to evaluating the model performance
31 and the parameter optimization results, the biogeochemical model equations should be reproduced in this
32 manuscript or in an appendix, rather than referring the reader to a different paper.

33 **Response:** The model code is published and freely available and the model equations, originally published in 2006,
34 have recently been republished in the Appendix of Laurent et al. (2017). The model has been used in well over a
35 dozen publications by our group and by hundreds of other researchers (the model is part of the widely used ROMS
36 distribution). We do not agree that it is necessary or frankly appropriate to republish the same equations which each
37 manuscript. This is also not common for other widely used models. In our revised manuscript, we added a specific
38 reference to the equation in the Appendix of Laurent et al. (2017) (P7 Lines 174).

39 Laurent, A., K. Fennel, W.-J. Cai, W.-J. Huang, L. Barbero, and R. Wanninkhof (2017), Eutrophication- induced
40 acidification of coastal waters in the northern Gulf of Mexico: Insights into origin and processes from a coupled
41 physical-biogeochemical model, Geophys. Res. Lett., 44, 946–956, doi:10.1002/2016GL071881.

42

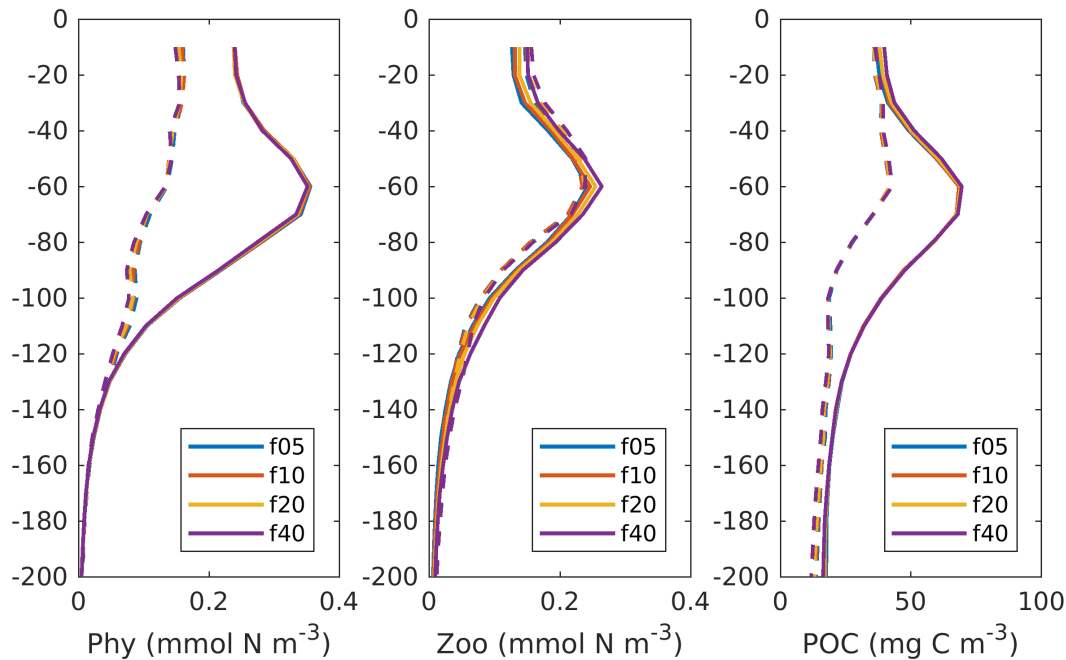
43 p. 8, Line 199: “Zooplankton and small detritus were assumed to amount to 10% of phytoplankton biomass and
44 the remaining fractions of POC attributed to large detritus.” Why is this assumption made? Is this assumption only
45 employed to define the initial condition?

46 **Response:** This assumption is also used for the open boundary conditions. For the biological model, the open
47 boundary conditions are usually unavailable. Here we assumed the zooplankton and small detritus accounted for
48 10% of phytoplankton following Gomez et al., 2018 in which 20% was assumed for a different biological model

49 in the Gulf of Mexico. We also do some sensitivity tests in the first year (2010) by perturbing this fraction to be
50 5%, 20%, and 40%. As shown in Figure 1, the choice of this fraction has little impact on the model results, e.g.
51 phytoplankton, zooplankton, and POC. In the revised manuscript, we also added a short comment on this
52 assumption (P8 Lines 188-189).

53
54 Gomez, F. A., Lee, S.-K., Liu, Y., Hernandez Jr., F. J., Muller-Karger, F. E., and Lamkin, J. T.: Seasonal patterns
55 in phytoplankton biomass across the northern and deep Gulf of Mexico: a numerical model study, *Biogeosciences*,
56 15, 3561–3576, <https://doi.org/10.5194/bg-15-3561-2018>, 2018

57



58
59

60 Figure 1. The simulated vertical profiles of phytoplankton, zooplankton, and POC from different sensitivity tests.
61 The solid lines represent median profiles while the dash lines represent interquartile range.

62

63 p. 8, Line 210: The 1D model setup is sensible, but more information is needed to understand, evaluate, and
64 reproduce the 1D model - Why is a 5 meter vertical resolution chosen in 1D and is the model sensitive to this
65 choice? - What are the units for the diffusion coefficient and why are these values chosen? They are substantially
66 higher than typical vertical diffusion coefficients in 3D models. - Are all of the parameters that are taken from the
67 3D model seasonally varying (the mixed layer depth, temperature, solar radiation, and NO₃ below 100 meters)? If
68 so, what the temporal frequency at which they are updated? - Why is the temperature and mixed layer depth
69 determined using values from the 3D model rather than the floats, which also have that data?

70 **Response:**

71 There are two main reasons why we chose 5 m. First, the vertical resolution in our BGC-Argo floats is 4-6 meters
72 in the upper 200 m. Second, a 5-m vertical resolution in the 1D model keeps the computational cost reasonable. As
73 stated in sections 3.4 and 3.5 of the manuscript, one parameter optimization experiment ran 36,000 model
74 simulations (30 simulations/generation * 300 generations*4 replications). It took us about one day to run a single

75 parameter optimization experiment and we performed 13 1D optimization experiments in total (A1-A4, B1-B4,
76 C1-C5). This is in addition to all the 3D model runs we performed.

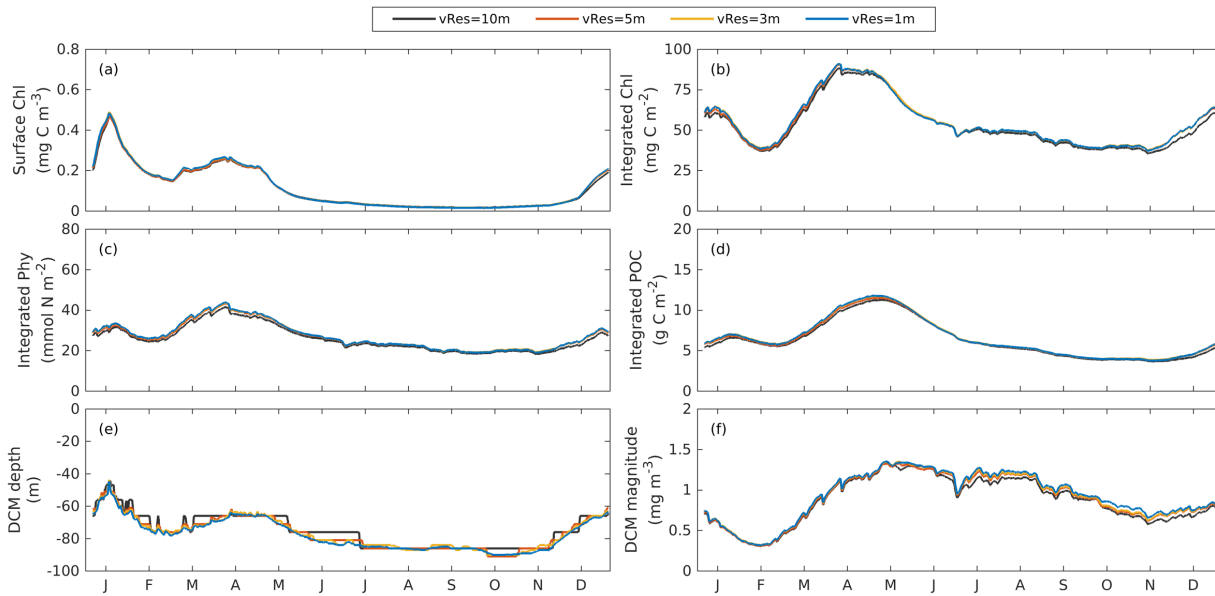
77 We are confident the vertical resolution is appropriate because we performed tests of the effect by using different
78 vertical resolutions including 10 m, 5 m, 3 m, and 1 m for optimization C4. As shown in the Figure 2 and 3 below,
79 the choice of vertical resolution has little impact on model results except for some small jumps in the DCM depth
80 (Figure 2e) and DCM magnitude (Figure 2) when the vertical resolution of 10 m is used.

81 The unit of the diffusion coefficient is $\text{m}^2 \text{day}^{-1}$ and its value was tuned such that our 1D and 3D models behave
82 similarly.

83 Finally, the physical input was obtained from daily output of the 3D model. Float data were not used as physical
84 inputs because of their low temporal resolution (~ 2 weeks).

85 We added explanations and comments on all of these issues in our revised manuscript (P8 Lines 198-207).

86 We also point to our responses to comments by Reviewer #1 under 3.2.
87



88
89 Figure 2. The simulated annual cycle of surface chlorophyll (a), vertically integrated chlorophyll (b), vertically
90 integrated phytoplankton (c), vertically integrated POC (d), and the depth (e) and magnitude (f) of the DCM by
91 using different vertical resolutions.

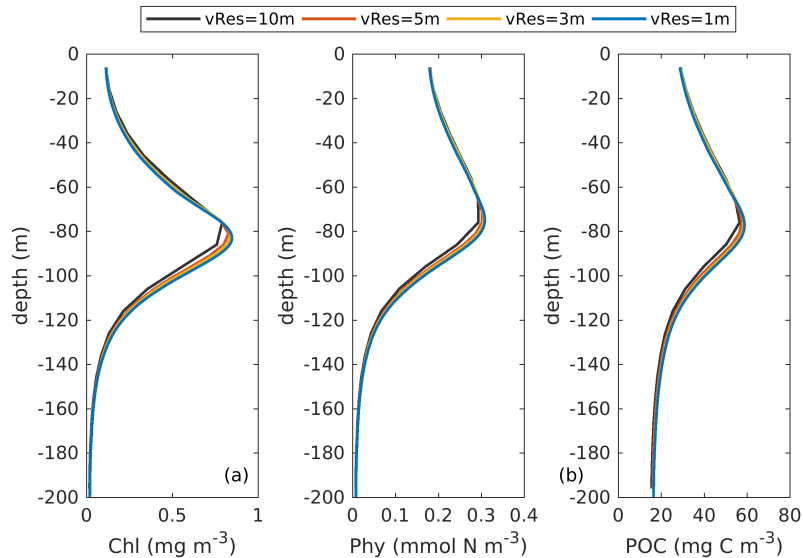


Figure 3. The simulated (colored lines) vertical profiles of chlorophyll, phytoplankton, and POC by using different vertical resolutions.

p. 11, Line 281: Why is the ratio of 0.1 between the sinking speed of the small and large detritus selected? How sensitive are the results to this choice?

Response: We refer to our response to Reviewer #1, comment on Pg 11 line 81-84, which we paste again here for sake of convenience:

These two parameters cannot be constrained simultaneously because they can compensate each other: an increase in the one parameter can be counteracted by a decrease in the other. This is a well-known and much discussed issue in the parameter optimization literature. Basically, there is no information in the available observations that allows to distinguish between the two. Including both parameters in the optimization will degrade the model's predictive skill. To solve this problem, one can either introduce more independent observations or prior knowledge by, e.g. fixing these parameters to their prior values or defining a link between these parameters. Generally, and also in this case, observations are insufficient to constrain all parameters and prior knowledge about the parameters has to be included. This is the common approach to addressing the underdetermination problem of parameter optimization in biological models.

In this study, the ratio of 0.1 was selected based on the prior values of the two parameters. Perturbing and estimating the ratio between two sinking velocities are equivalent to letting both parameters (w_{SDet} and w_{LDet}) into optimization and may degrade model's predictive skills. Without additional information about the depth distribution of S_{det} and L_{det} , which is not available, the ratio cannot be constrained.

The underdetermination problem and the practice of incorporating prior knowledges is also discussed on P20, L10-28 of our original manuscript.

4. Optimization of 1D model

This section is well written and clear. The discussion of the differences between the surface chlorophyll and vertical profiles is particularly clear and interesting.

19 **Response:** Thank you for this comment.

20

21 p. 13, Line 329: “Unlike phytoplankton, the observations show that the POC concentrations are 19 mg C m⁻³ at
22 about 200 m depth because of the existence of detritus (Figure 4c).” What is the evidence that the POC is in the
23 detritus class rather than zooplankton? This point is not supported, but is used later to discriminate between models.

24 **Response:** We revised this as follows: “... *the POC concentrations are 19 mg C m⁻³ at about 200 m depth because*
25 *of the existence of detritus, or zooplankton, or both*”. We also revised the P15 L70-71 of original manuscript to
26 *“In contrast to the observations where the phytoplankton’s contribution is neglectable (Figure 4), the simulated*
27 *POC at 200 m is dominated by phytoplankton (49%)”*.

28

29 Section 4.2: In the section for each experiment, remind the reader what data is used the optimization and which
30 parameters are included in the parameter optimization

31 **Response:** As stated already in response to Reviewer 2, we revised as suggested.

32

33 Could you plot the mixed layer depth of the 1D model for comparison to the DCM depth? In the 1D model, the
34 mixed layer depth is the main physical control. One option would be to plot the mixed layer depth in figure 3e.

35 **Response:** Since the Figure 3e would be busy with a plot of the mixed layer, we plot the seasonal mean levels of
36 the mixed layer in Figure 4 and hope that would convey the information this reviewer was looking for.

37

38 The supplemental figure S1 shows that even the corrected satellite data does not capture the seasonality observed
39 by the floats. One sentence here describing the differences that remain between the floats and corrected OC-CCI
40 could help us to better assess why experiment A in particular does not capture the seasonality.

41 **Response:** In the experiment A, the satellite estimates of surface chlorophyll was used in parameter optimization
42 and the model results were compared with the satellite data in the Figure 3a. The differences between the satellite
43 and float data would not be a reason for experiment A not capturing the peak of satellite surface chlorophyll. It
44 could be a result of many factors and might be improved by assigning a higher weight on the peaks of surface
45 chlorophyll. However, studying the peaks of surface chlorophyll was not the purpose in this study. Nonetheless,
46 the parameter optimization resulted in a large improvement in surface chlorophyll in the experiment A.

47

48 p. 15, Line 375: “Although a slight increase in the misfit occurs for the surface chlorophyll (~5%),” Is the increase
49 of 5% relative to experiment B?

50 **Response:** The slight increase here was relative to the base case. The full sentence in the original manuscript is
51 *“Although a slight increase in the misfit occurs for the surface chlorophyll (~5%), the total misfit is reduced by*
52 *75% compared to the base case.”* We hope this is clear.

53

54 Table 2: In the caption, explain what the dashes in the table mean. In the cases where the parameters are not included
55 in the optimization, are the values that are presented in table 1 used? It would be helpful to the reader if the
56 experiment that is discussed in the text is highlighted. Since different parameters are used in the 3D experiment,
57 include additional lines in this table for the parameters that are used in the 3D experiment.

58 **Response:** Thanks for this comment. We revised as suggested.

59

60 Figure 3: Include what data is used for each experiment in the figure caption. Could error bars be added to the
61 observational points in this figure?

62 **Response:** Yes, we revised as suggested.

63
64 Figure 4: What do the error bars represent? Are they the interquartile range?

65 **Response:** Yes, they are interquartile range. We now state this explicitly in the caption of Figure 4.

66
67 5. 3D biogeochemical model

68 p. 16, Line 421: How were the parameters that were modified manually chosen? It would be useful to provide more
69 discussion of this choice.

70 **Response:** Same as comment “5. 3D biogeochemical model” by Reviewer 1 and same response. We paste it again
71 here for sake of convenience:

72 We did manual modifications because when the resulting parameters were directly applied, the model-data
73 agreement in 3D models was not as well as in 1D models in some aspects, but the most important features were
74 well preserved. In experiment C, chlorophyll concentrations in the upper layer of 3D model were lower than the
75 1D model and farther away from observations. This might be a result of differences between 1D and 3D models
76 and has been also reported in other studies (e.g. Kane et al., 2011; Hoshiba et al., 2018). However, the depth of the
77 DCM and the non-zero POC concentrations at 200 m with appropriate contributions from each component were
78 well preserved. We therefore did some tests manually by tuning one or two parameters and final set the KNH4
79 to 0.01 in order to have a better agreement with respect to observations. All of these modifications were based on
80 our tests.

81 In our case, although the 1D parameter sets could not be used in 3D models directly, they were sufficient to
82 reproduce the main features as in 1D models and largely simplified the following subjective tuning of 3D models
83 by limiting the number of parameters to be adjusted.

84 We included more explanations for the manual modifications (P16 Lines 400-411) and discussion (P20-21 Lines
85 522-530) in our revised manuscript.

86
87 p. 17, Line 442: Here the authors point to specific parameters that were inappropriate, but on p. 10, Line 246 the
88 authors say that parameters are not allowed to exit a predefined range (which is shown in table 1). This seems
89 inconsistent given that the method could have excluded inconsistent values. Could this difference be explained in
90 more detail?

91 **Response:** We think there might be a misunderstanding here. The predefined range of parameters was a collection
92 of their values that had been used in other studies, models, and ecosystem regimes. That means not all parameter
93 values within this range are appropriate for our model. The parameter optimization is therefore to search for an
94 optimal parameter set within this predefined range by minimizing the misfit between model and observations.
95 However, the parameter optimization cannot constrain all parameters (e.g. producing the inappropriate estimates)
96 because of insufficient observations, which is referred to as the underdetermination problem (see earlier responses
97 here and for Reviewer 1). For instance, in our experiment B, the parameter optimization fitted our model to
98 chlorophyll observations but sacrificed other aspects of the model’s performance which were degraded, e.g. the
99 vertical profiles of phytoplankton. That is why we said the estimates of the maximum ratio between chlorophyll
00 and phytoplankton ($\theta_{max}= 0.0158$) in experiment B was inappropriate. An appropriate estimate of this parameter
01 requires more independent observations, e.g. of phytoplankton that we used in the experiment C.

02
03 Section 5.1: The authors state that the 3D model does not perform well in coastal regions and therefore choose to
04 exclude those regions from the model evaluation. This may be justified based on the statement in section 2 that

05 there is little cross-shelf exchange in the Gulf of Mexico. However, this point should be discussed in more detail
06 in order to justify ignoring the shelf. In particular, it is important to discuss the extent to which nutrients are supplied
07 to the oligotrophic regions from either the shelf or the open ocean boundary. What is the importance of the
08 boundaries relative to the biogeochemical cycling in the interior? In a 3D model, the boundaries could be very
09 important for setting the primary production in the oligotrophic region.

10 **Response:** Firstly, we excluded coastal regions because we have no float data in coastal regions used for parameter
11 optimization and model validation. All parameter optimization experiments in this study were designed for
12 modelling the deep ocean part of the Gulf of Mexico. In our revised manuscript, we clarified this, see P16-17 Lines
13 419-421.

14 Secondly, if we define the boundary between coastal regions and open ocean as 1,000 m, the DIN fluxes
15 ($\text{NO}_3 + \text{NH}_4$) across the 1,000 m isobath is a sink for the open ocean and nearly balanced by the inputs from open
16 boundaries. Specifically, for the upper 200 m where the primary production occurs, the amount of DIN transported
17 is $2.7 \times 10^{11} \text{ mol N yr}^{-1}$ (sink) from the open ocean into coastal region and $2.1 \times 10^{11} \text{ mol N yr}^{-1}$ (source) from open
18 boundaries. The primary production in the deep part of the Gulf of Mexico is $10.6 \times 10^{11} \text{ mol N yr}^{-1}$ (sink for DIN)
19 which is mainly supported by the vertical transport and interior nitrogen recycle in the upper 200 m.

20
21 p. 18, Line 451: What is meant by “different spatio-temporal scales between the two model versions”? This point
22 seems important and could be clarified. Is it referring to time stepping, resolution, retention in a 1D location, or the
23 presence of a seasonal cycle?

24 **Response:** The different spatial-temporal scales refer to a lot of factors here. The 1D model is configured in a
25 single station while the 3D model covers the whole Gulf of Mexico. In the vertical direction, the 1D model only
26 simulates the upper 200 m but the 3D model has the whole water column. For temporal scales, the 1D model is
27 simulated for one year but the 3D model runs for 6 years from 2010 to 2016. The model steps are also different
28 between the 1D and 3D models. In our revised manuscript, we removed these sentences but as suggested, we
29 clarified when we talk about the differences between 1D and 3D models (P16 Lines 400-403).

30
31 p. 19, Line 479: “cannot” should be “can not”

32 **Response:** Revised as suggested.
33
34
35
36
37
38
39

1 **Assessing the value of BGC Argo profiles versus ocean colour observations** 2 **for biogeochemical model optimization in the Gulf of Mexico**

3 Bin Wang¹, Katja Fennel¹, Liuqian Yu^{1,2}, Christopher Gordon¹

4 ¹Department of Oceanography, Dalhousie University, Halifax, Nova Scotia, Canada

5 ²Department of Mathematics, The Hong Kong University of Science and Technology, Kowloon, Hong Kong

6 **Correspondence to:** Bin Wang (Bin.Wang@dal.ca)

7 **Abstract.** Biogeochemical ocean models are useful tools but subject to uncertainties arising from simplifications,
8 inaccurate parameterization of processes, and poorly known model parameters. Parameter optimization is a
9 standard method for addressing the latter but typically cannot constrain all biogeochemical parameters because of
10 insufficient observations. Here we assess the trade-offs between satellite observations of ocean colour and
11 biogeochemical (BGC) Argo profiles, and the benefits of combining both observation types, for optimizing
12 biogeochemical parameters in a model of the Gulf of Mexico. A suite of optimization experiments is carried out
13 using different combinations of satellite chlorophyll and profile measurements of chlorophyll, phytoplankton
14 biomass, and particulate organic carbon (POC) from autonomous floats. As parameter optimization in 3D models
15 is computationally expensive, we optimize the parameters in a 1D model version, and then perform 3D simulations
16 using these parameters. We show first that the use of optimal 1D parameters, with a few modifications, improves
17 the skill of the 3D model. Parameters that are only optimized with respect to surface chlorophyll cannot reproduce
18 subsurface distributions of biological fields. Adding profiles of chlorophyll in the parameter optimization yields
19 significant improvements for surface and subsurface chlorophyll but does not accurately capture subsurface
20 phytoplankton and POC distributions because the parameter for the maximum ratio of chlorophyll to phytoplankton
21 carbon is not well constrained in that case. Using all available observations leads to significant improvements of
22 both observed (chlorophyll, phytoplankton, and POC) and unobserved (e.g. primary production) variables. Our
23 results highlight the significant benefits of BGC Argo measurements for biogeochemical parameter optimization
24 and model calibration.

25 **1. Introduction**

26 Oceanic primary production forms the basis of the marine food web and fuels the biological pump, which
27 contributes to the sequestration of atmospheric CO₂ in the ocean's interior thus mitigating global warming. An
28 accurate quantification of primary production and biological carbon export is therefore important for our
29 understanding of the marine carbon cycle and for predicting how carbon cycling and marine ecosystems will
30 interact with climate change.

31 Direct observations of primary production and export flux are relatively sparse because of the cost and effort
32 involved in measuring these fluxes. Numerical models can complement sparse observations. Well validated and
33 calibrated models are useful tools for hindcasting and nowcasting past and present biogeochemical fluxes and are
34 the most common tool for projecting future changes.

35 In recent years, many biogeochemical models with different complexities, ~~ranging from three to more than~~
36 ~~thirty biological state variables~~, have been developed to study ocean biogeochemical processes. Regardless of their
37 complexities, the performance of these models is highly dependent on the appropriate choice of model parameter
38 values (e.g. maximum growth, grazing and mortality rates), most of which are poorly known. ~~Some parameter~~
39 ~~choices are informed by laboratory experiments (e.g. light and nutrient dependence of phytoplankton growth),~~
40 ~~although isolated cultures in the lab may not be representative of the behavior of natural communities. Other~~
41 ~~parameters cannot be directly determined (e.g. mortality rates). Choosing appropriate parameter values becomes~~
42 ~~more challenging as model complexity grows because the number of parameters increases exponentially with the~~
43 ~~number of state variables (Denman, 2003).~~ A standard method for choosing these parameters is optimization, a
44 process by which the misfit between model results and available observations is minimized by iteratively varying
45 parameters (Matear, 1995; Prunet et al., 1996a, 1996b; Fennel et al., 2001; Friedrichs et al., 2007; Kuhn et al.,
46 2015, 2018). However, even formal optimization typically cannot constrain all biogeochemical parameters (i.e.
47 provide optimal parameter estimates with relatively small uncertainties) because of insufficient information in the
48 available observations (Matear, 1995; Fennel et al., 2001; Ward et al., 2010; Bagniewski et al., 2011). For example,
49 Matear (1995) used a so-called simulated annealing algorithm to optimize three different ecosystem models and
50 found that even for the simplest nutrient-phytoplankton-zooplankton model, not all independent parameters could
51 be constrained well, leaving the others with large uncertainty ranges. A more recent study reported that the lack of

52 zooplankton observations led to poor accuracy of the optimized zooplankton-related parameters when using a suite
53 of Lagrangian-based observations during the North Atlantic spring bloom (Bagniewski et al., 2011). A broader
54 suite of observation types should be favourable to parameter optimization although complications can arise. For
55 example, when optimizing a suite of 1D models for the Mid-Atlantic Bight, the use of satellite POC observations
56 in addition to satellite chlorophyll did not yield further improvements in model-data fit but degraded the
57 representation of chlorophyll (Xiao and Friedrichs, 2014a).

58 Typically surface ocean chlorophyll from satellite is the main source of observations for model validation (e.g.
59 Doney et al., 2009; Gomez et al., 2018; Lehmann et al., 2009) and parameter optimization (Prunet et al., 1996a;
60 Xiao and Friedrichs, 2014a, 2014b), supplemented by other observation types as available. However, satellites only
61 see the ocean surface and do not resolve the vertical distribution of chlorophyll. This is especially problematic in
62 oligotrophic regions where the deep chlorophyll maximum (DCM) is relatively deep and hardly observed by the
63 satellite (Cullen, 2015; Fennel and Boss, 2003). In addition, although chlorophyll has long been used as a proxy of
64 phytoplankton biomass and to estimate primary production based on some assumptions (Behrenfeld and Falkowski,
65 1997), it is not a direct measure of carbon-based phytoplankton biomass. The ratio of chlorophyll-to-phytoplankton
66 carbon varies by at least an order of magnitude due to physiological responses of phytoplankton to their ambient
67 environment (e.g. nutrients, light, and temperature) (Cullen, 2015; Fennel and Boss, 2003; Geider, 1987). Changes
68 in chlorophyll may result from physiologically induced modifications of the chlorophyll-to-phytoplankton ratio
69 rather than actual changes of phytoplankton biomass (Fommervault et al., 2017; Mignot et al., 2014). Satellite
70 surface chlorophyll alone is therefore likely insufficient for model validation and for constraining biogeochemical
71 models via parameter optimization.

72 Recent advances in autonomous platforms and sensors have opened opportunities for simultaneous
73 measurement of several biological and chemical properties throughout the upper ocean with high resolution, over
74 broad spatial scales and for sustained periods (Roemmich et al., 2019). In particular, the biogeochemical (BGC)
75 Argo program (Johnson and Claustre, 2016; Roemmich et al., 2019) will provide temporally evolving 3D
76 information on biogeochemical variability at previously unobserved scales. Here we assess to what degree
77 observations of chlorophyll fluorescence and particle backscatter from Argo profiles improve the prospects of
78 optimizing a biogeochemical model for the Gulf of Mexico.

79 Since the high computational cost and storage demands of 3D models make direct application of most
80 parameter optimization techniques difficult (but see Mattern et al., 2012; Mattern and Edwards, 2017; Tjiputra et
81 al., 2007 for exceptions), they are typically applied in computationally efficient 1D models before using the
82 resulting parameters in 3D version (e.g. Hoshiba et al., 2018; Kane et al., 2011; Kuhn and Fennel, 2019; Schartau
83 and Oschlies, 2003). We follow the latter approach here.

84 The main objective of this study is to assess the added value of bio-optical profile information from Argo
85 floats for biogeochemical model optimization in the Gulf of Mexico. We first examine the feasibility of improving
86 the 3D model by applying the optimal parameters from 1D model optimizations **with some minor manual**
87 **modifications**. We find that the gains from the 1D optimizations transfer to the 3D version. Then, by using different
88 combinations of satellite and float observations we show that parameters optimized with respect to satellite data
89 cannot reproduce subsurface distributions unless the float observations (i.e. chlorophyll, phytoplankton, and POC)
90 are also used.

91 **2. Study region**

92 The Gulf of Mexico (GOM) is a semi-enclosed marginal sea (Figure 1) which is characterized by eutrophic
93 coastal waters on the northern shelf and an oligotrophic deep ocean. The high productivity in the northern coastal
94 region is fueled by large nutrient and freshwater inputs from the Mississippi and Atchafalaya Rivers. The large
95 nutrient load and strong stratification driven by Mississippi and Atchafalaya River inputs lead to summer hypoxia
96 and ocean acidification in bottom waters on the northern shelf (Laurent et al., 2017; Yu et al., 2015), but nutrient
97 export across the shelf break into the open Gulf is minor (Xue et al., 2013).

98 The deep ocean of the GOM is oligotrophic. Previous satellite-based studies have revealed a clear seasonal
99 cycle in surface chlorophyll with highest concentrations in winter and lowest in summer (Martínez-López and
00 Zavala-Hidalgo, 2009; Muller-Karger et al., 1991, 2015). Thanks to advances in autonomous profiling technology,
01 recent studies based on simultaneous measurements of subsurface chlorophyll and backscatter have demonstrated
02 that the seasonal variability of surface chlorophyll might be a result of the vertical redistribution of subsurface
03 chlorophyll and/or physiological response to solar radiation of phytoplankton (Fommervault et al., 2017; Green et
04 al., 2014).

05 3. Methods

06 3.1. Biological observations

07 Monthly averaged satellite chlorophyll from the Ocean-Colour Climate Change Initiative project (OC-CCI,
08 <https://www.oceancolour.org>) with a spatial resolution of 4 km from 2010 to 2015 was used for model validation
09 and parameter optimization. These data were provided by the European Space Agency (ESA), which produced a
10 set of validated and error-characterised global ocean-color products by merging SeaWiFS (Sea-viewing Wide
11 Field-of-view Sensor), MODIS (Moderate-resolution Imaging Spectroradiometer), MERIS (medium-spectral
12 resolution imaging spectrometer), and VIIRS (Visible Infrared Imaging Radiometer Suite) products.

13 In addition to the satellite-based measurements, bio-optical measurements from six autonomous profiling
14 floats were used (Figure 1), which were deployed by the Bureau of Ocean Energy Management (BOEM) and
15 operated in the deep GOM from 2011 to 2015. These floats were equipped with a CTD and bio-optical sensors to
16 collect biweekly profiles of temperature, salinity, chlorophyll, and backscatter at 700 nm ($bbp700$ (m^{-1})) from the
17 surface to 1000 m depth (see Fommervault et al., 2017 and Green et al., 2014 for more details). Chlorophyll was
18 derived from fluorescence based on the sensor manufacturer's calibrations and compared with the satellite
19 estimates of surface chlorophyll. While the surface chlorophyll measurements from the floats and the satellite
20 estimates both showed a typical seasonal cycle and were highly correlated ($R^2=0.74$; see Figures S1 and S2a in the
21 Supplement), the satellite underestimated the float-measured chlorophyll concentrations in winter (Figure S1c).
22 Satellite estimates were therefore corrected following the regression equation shown in Figure S2a.

23 The backscatter sensor carried by the floats provided the volume scattering function at a centroid angle of
24 140° and a wave length of 700 nm ($\beta(140^\circ, 700nm)$ $m^{-1} sr^{-1}$). The profiles were filtered (Briggs et al., 2011) to
25 remove spikes and then converted into $bbp700$ following Green et al. (2014). After that, profiles of $bbp700$ were
26 converted into $bbp470$ based on a power law (Boss and Haëntjens, 2016) to obtain the phytoplankton ($mmol N m^{-3}$)
27 and POC ($mg C m^{-3}$) estimates:

$$28 \quad bbp(\lambda_1) = \left(\frac{\lambda_1}{\lambda_2}\right)^{-\gamma} bbp(\lambda_2), \quad (1)$$

$$29 \quad Phy = 30100 \times (bbp470 - 76 \times 10^{-5}) \frac{1}{12 \times 6.625}, \quad (2)$$

30
$$\log_{10}(POC) = 1.22 \times \log_{10}(bbp470) + 5.15. \quad (3)$$

31

32 where λ_1 and λ_2 represented the measured wavelength, and γ was estimated as 0.78 based on the global
33 measurements. The relationships for phytoplankton (Martinez-Vicente et al., 2013; equ. 2) and POC (Rasse et al.,
34 2017; equ. 3) were obtained from a data set for the Atlantic Ocean that covered a wide range of oceanographic
35 regimes from eutrophic to oligotrophic ecosystems. The scale factors of 12 and 6.625 in equ. 2 represented the
36 molecular weight of carbon and the Redfield ratio to convert phytoplankton concentrations from mg C m^{-3} to mmol
37 N m^{-3} . The intercept 76×10^{-5} in equ. 2 represented the background backscatter of nonalgal detritus, which
38 based on Behrenfeld et al. (2005) was the backscatter value when chlorophyll was zero. However, in this study,
39 the most majority (87%) of *bbp470* in the upper 200m was below the intercept and the resulting phytoplankton
40 concentrations were therefore close to zero, which is unrealistic in the Gulf of Mexico. Therefore, the satellite
41 estimate of *bbp670* from OC-CCI was converted into *bbp700* and compared with the float measurements.
42 Compared to surface chlorophyll, surface *bbp700* has a less distinct seasonal cycle (Figure S3). For example, the
43 coefficient of variation, defined as the ratio between standard deviation and mean to show the extend of variability,
44 is much lower for *bbp700* (0.09 and 0.07 for floats and satellite, respectively) than for chlorophyll (0.31 and 0.26
45 for floats and satellite, respectively). The float *bbp700* is weakly correlated with the satellite estimates ($R^2=0.11$)
46 and generally lower by a factor of 0.45 than the satellite estimates (Figure S2b). The *bbp700* profiles were therefore
47 multiplied by 2.2 before being converted to *bbp470*. As a result, the mean value of the *bbp470* ($88 \times 10^{-5} \text{ m}^{-1}$)
48 is close to the intercept in equ.2 when chlorophyll went to zero. Furthermore, the resulting concentrations of
49 phytoplankton biomass and POC as well as the ratio of chlorophyll to phytoplankton biomass are reasonable (please
50 see figures 4 and 10). This gave us confidence in our conversion process for float backscatter and our choice of
51 empirical equations relating backscatter to phytoplankton and POC.

52 3.2. 3D model description

53 The physical model was configured based on Regional Ocean Modeling System (Haidvogel et al., 2008;
54 ROMS, <https://www.myroms.org>) for the Gulf of Mexico (Figure 1). The model has a horizontal resolution of 6~7
55 km and 36 terrain-following sigma layers with refined resolution near the surface and bottom. The model solved
56 the horizontal and vertical advection of tracers using the Multidimensional positive definitive advection transport

57 algorithm (MPDATA, Smolarkiewicz and Margolin 1998). Horizontal viscosity and diffusivity were parameterized
58 by a Smagorinsky-type formula (Smagorinsky, 1963), and vertical turbulent mixing was calculated by the Mellor-
59 Yamada 2.5-level closure scheme (Mellor and Yamada, 1982). Bottom friction was specified by a logarithmic drag
60 formulation with a bottom roughness of 0.02 m. The model was forced by 3-hourly surface heat and freshwater
61 fluxes, 6-hourly air temperature, sea level pressure and relative humidity, and 10-m winds from the European
62 Centre for Medium-Range Weather Forecast ERA-Interim product with a horizontal resolution of 0.125° (ECMWF
63 reanalysis, <https://www.ecmwf.int/en/forecasts/datasets/reanalysis-datasets/era-interim>). A bulk parameterization
64 was applied to calculate the surface net heat fluxes and wind stress. The model was one-way nested inside the 1/12°
65 data-assimilative global HYCOM/NCODA (<https://www.hycom.org>). Tidal constituents were neglected in the
66 model.

67 The biogeochemical model used a 7-component model (Fennel et al., 2006) to simulate the nitrogen cycle in
68 the water column. The model described the dynamics of two species of dissolved inorganic nitrogen (nitrate, NO₃,
69 and ammonium, NH₄), one function of phytoplankton (Phy), chlorophyll (Chl) as a separate state variable which
70 allowed photo-acclimation based on the model of Geider et al. (1997), one function of zooplankton (Zoo), and two
71 pools of detritus (i.e. small suspended detritus, SDeN, and large fast-sinking detritus, LDeN). Water-sediment
72 interactions were simplified by an instantaneous remineralization parameterization, where detritus sinking out of
73 water column immediately resulted in a corresponding influx of ammonium into the bottom layer. Detailed
74 descriptions of the model equations can be found in Fennel et al. (2006) and Laurent et al. (2017). The biological
75 model parameters are listed in Table 1.

76 The model received freshwater, nutrients (NO₃ and NH₄) and organic matter inputs from major rivers along
77 the Gulf coast. Freshwater and nutrients from the Mississippi and Atchafalaya rivers were prescribed based on the
78 daily measurements by the US Geological Survey river gauges. River particulate organic nitrogen (PON) was
79 assigned to the small detritus pool and determined as the difference between total Kjeldahl nitrogen and ammonium
80 (Fennel et al., 2011). Other rivers utilized the climatological estimates of freshwater, nutrients, and PON as in Xue
81 et al. (2013).

82 Initial and open boundary conditions for NO₃ were specified by applying an empirical relationship between
83 NO₃ and temperature, derived from the World Ocean Atlas (WOA; Figure S4a), that was applied to the temperature

84 fields from HYCOM/NCODA. Analogously, empirical relationships between chlorophyll and density (Figure
85 S4b), phytoplankton and density (Figure S4c), and POC and density (Figure S4d) were obtained from the median
86 profiles of the bio-optical floats and used to derive initial and boundary conditions for these variables. Zooplankton
87 and small detritus were assumed to amount to 10% of phytoplankton biomass and the remaining fractions of POC
88 attributed to large detritus. Sensitivity tests showed that changing these allocations had little impact on our model
89 results.

90 A 6-year (5 January 2010 – 31 December 2015) hindcast was performed that included the period of operation
91 of the bio-optical floats. The first year was considered model spin-up and the next five years are discussed.

92 3.3. 1D model description

93 As optimizing a 3D biogeochemical model is computationally expensive, it was more practical to perform
94 the optimization using a reduced-order model surrogate. A surrogate can be a coarser resolution model, a simplified
95 model, or a reduced-dimension model. In this study, a 1D model was used to optimize the biological parameters of
96 the 3D model. This approach has been successfully used previously (Hoshiba et al., 2018; Kane et al., 2011;
97 Oschlies and Schartau, 2005).

98 The 1D model, which is similar to that used by Lagman et al. (2014) and Kuhn et al. (2015), covered the
99 upper 200 m of the ocean with a vertical resolution of 5 m and was configured at one location in the open Gulf (see
00 Figure 1). This relatively fine vertical resolution was used because it was close to that of our BGC-Argo floats
01 (4–6m in upper 200m) and was much higher than the 3D model whose vertical resolution varies from a few meters
02 near the surface to about 50 m near at 200 m depth around the 1D station. In the vertical direction, the water column
03 was divided into two layers: the turbulent surface layer and a quiescent layer below. A higher diffusion coefficient
04 ($K_{Z1} = \max(H_{MLD}^2/400, 10)$, in unit of $m^2 \cdot day^{-1}$) was applied in the turbulent surface layer and a lower
05 diffusion coefficient ($K_{Z2} = K_{Z1}/2$) was assigned to the quiescent bottom layer. The interface between these two
06 layers was determined by the mixed layer depth (H_{MLD} , in unit of m), defined as the depth where the temperature
07 was 5°C lower than at the surface, and was obtained from daily outputs of the 3D model. The model was integrated
08 in time using the Crank-Nicolson scheme for vertical turbulent mixing and an implicit time-stepping scheme for
09 the biogeochemical tracers, which were treated identically to the 3D model. Some of the biogeochemical
10 parameterizations required input of temperature and solar radiation, which were also taken from the 3D model. As

11 the 1D model did not consider horizontal and vertical advection, NO₃ below 100 m was nudged to that from the
 12 3D base simulation with a nudging time scale of 20 days. The 1D model was run for the year 2010 repeatedly for
 13 three cycles, with the first two were model spin-up and the last annual cycle used to calculate the misfit between
 14 model and observations.

15 **3.4. Parameter optimization method**

16 The evolutionary algorithm described by Kuhn et al. (2015, 2018) was used to search for optimal model
 17 parameters by minimizing the misfit between model and observations. The misfit was measured by the following
 18 cost function:

19

$$20 \quad F(\vec{p}) = \sum_{v=1}^V F_v(\vec{p}), \quad (4)$$

21

$$22 \quad F_v(\vec{p}) = \frac{1}{N_v \sigma_v^2} \sum_{i=1}^{N_v} (\hat{y}_{i,v} - y_{i,v}(\vec{p}))^2, \quad (5)$$

23

24 where \vec{p} represented the parameters vector, V was the number of different observation types, N_v was the number
 25 of observations for each variable, $F_v(\vec{p})$ was the misfit for observation type v measured as the mean-square
 26 difference between observations (\hat{y}) and corresponding model estimates ($y(\vec{p})$). The cost function $F_v(\vec{p})$ was
 27 normalized by the standard deviation of each variable type (σ_v) in order to remove the effect of different units.

28 The algorithm is inspired by the rules of natural selection. Following Kuhn et al. (2015), an initial parameter
 29 population of 30 parameter vectors was randomly generated within a predefined range of parameters (see Table 1).
 30 The model was evaluated for each parameter vector and the resulting cost function was calculated. For this initial
 31 generation and each of the following generations, the half of the population with the lower misfit survived into the
 32 next generation. The other half was regenerated through a recombination of survivors in a process analogous to
 33 genetic crossover. In addition, each newly generated population was subject to random mutations by multiplying
 34 the parameter values by a random value between 0 and 2. Parameter values exceeding the predefined range were
 35 replaced by their corresponding minimum or maximum limits to avoid unrealistic values. The above procedure was

36 performed iteratively for 300 generations to reach the minimum of the cost function, which corresponded to the
37 optimal parameter set.

38 Previous parameter optimization studies have shown that it is difficult to constrain all model parameters even
39 for very simple ecosystem models because the information content of available observations is typically insufficient
40 (Matear, 1995; Fennel et al., 2001; Ward et al., 2010). Here we conducted sensitivity tests to identify the parameters
41 that were most sensitive to the available observations and chose a subset of these to be optimized. In the **base case**,
42 all parameters were at their initial guess values obtained from the previous literature and some initial tuning (Table
43 1). Then the **test cases** were run multiple times by incrementally changing one parameter at a time to be the
44 minimum, the first, second and third quartile, and the maximum of its corresponding range while setting the other
45 parameters to their initial guess value (Table 1). The sensitivity was measured as the sum of a normalized absolute
46 difference between the base case (y_{Base}) and the test case (y_{Test})

47

48

$$Q(y, \vec{p}) = \frac{1}{m} \sum_{i=1}^m \frac{1}{n} \sum_{j=1}^n \frac{|y_{Base} - y_{Test}|}{y_{Base}} \quad (6)$$

49

50 where m is the number of parameter increments (here 5) and n is the number of base-test pairs **consisting** of all 1D
51 model grid cells throughout the whole simulation period for all variables to be compared.

52

53 Results of the sensitivity analysis are shown in Figure 2, where parameters are ranked by sensitivity with
54 respect to chlorophyll (Figure 2a) and the sum of chlorophyll, phytoplankton, and POC (Figure 2b). POC is the
55 sum of phytoplankton, zooplankton, and small and large detritus.

56

3.5. Parameter optimization experiments

57

58 For the parameter optimization of the 1D model, satellite chlorophyll within a 3×3 pixel (12 km×12 km area)
59 around the 1D station and monthly climatological profiles from the BGC-Argo floats were used. **For the
60 climatological profiles, all float profiles in the Gulf were averaged because the deep Gulf of Mexico is homogenous
61 horizontally and only few profiles were available in the immediate vicinity of the 1D station.**

62

63 To assess the effects of the optimization with respect to the different observation types, we conducted three
64 groups of experiments in which (A) surface satellite chlorophyll only, (B) surface satellite chlorophyll and float

62 profiles of chlorophyll, and (C) surface satellite chlorophyll and float profiles of chlorophyll, phytoplankton, and
 63 POC were used. For each of these three groups, four to five optimizations were conducted starting with the three
 64 most sensitive parameters and then adding one more parameter at a time (Table 2) guided by the sensitivity analysis
 65 with respect to observed variables they used. Specifically, groups A and B were based on the sensitivity analysis
 66 with respect to chlorophyll, while group C was based on sensitivity analysis with respect to the sum of chlorophyll,
 67 phytoplankton, and POC. Each optimization was replicated four times. The optimization with smallest model-data
 68 misfit within each group was then used. Prior tests have shown that the available observations cannot
 69 simultaneously constrain the sinking rates of small and large detritus (w_{SDet} and w_{LDet}) because an increase in one
 70 parameter can be counteracted by a decrease in the other. Therefore, a constant ratio of 0.1 between these two
 71 parameters ($w_{SDet} = 0.1 \times w_{LDet}$) was imposed based on their prior values and only one of the two was optimized. In
 72 groups A and B, the aggregation parameter τ was fixed at 0.05 because prior tests generated unreasonably high
 73 values for this parameter.

74 We report two different metrics of misfits for these groups of experiments. The first metric, which we refer
 75 to as the case-specific cost function value, is based on the optimized observations in a given experiment and was
 76 minimized by the optimization algorithm, i.e.

$$77 \quad F_A(\vec{p}) = F_{SurfCHL}(\vec{p}), \quad (7)$$

$$78 \quad F_B(\vec{p}) = F_{SurfCHL}(\vec{p}) + F_{CHL}(\vec{p}), \text{ and} \quad (8)$$

$$79 \quad F_C(\vec{p}) = F_{SurfCHL}(\vec{p}) + F_{CHL}(\vec{p}) + F_{Phy}(\vec{p}) + F_{POC}(\vec{p}). \quad (9)$$

80
 81
 82
 83
 84 However, the models with lower case-specific misfit do not necessarily have better predictive skill in reproducing
 85 the unoptimized observations because of the so-called overfitting problem, e.g. the model might be tuned to
 86 reproduce optimized observations through wrong mechanisms (Friedrichs et al., 2006). To account for this, a
 87 second metric referred to as the total misfit is given by equ. 9. For group C, the second metric is the same as the

88 case-specific cost function. For groups A and B, the total misfit metric allows us to assess improvements in the
89 model's predictive skill to represent unoptimized fields.

90 **4. Optimization of 1D models**

91 **4.1. Observations and base case**

92 To provide context for the evaluation of our optimization experiments, the observations and the base case
93 will be described first. As shown in Figure 3a, the observed surface chlorophyll shows a clear seasonality with the
94 high concentrations in winter and low concentrations in summer. In the base case, the simulated surface chlorophyll
95 fits observations well. Unlike the surface chlorophyll, the **observed** integrated chlorophyll as well as the
96 phytoplankton and POC over the upper 200 m tend to be more constant with much less seasonality (Figure 3b-d).
97 This has been reported by Fommervault et al. (2017) who attributed the seasonality of surface chlorophyll to the
98 vertical redistributions of subsurface chlorophyll and/or photoacclimation, rather than real changes in biomass.

99 The DCM is a ubiquitous phenomenon in the oligotrophic regions **and can form independently of the biomass**
100 **maximum (Cullen, 2015; Fennel and Boss, 2003). In this study, we define the DCM depth as where the maximum**
101 **of subsurface chlorophyll is.** Observations detect a predominant DCM at around 60-100m depth throughout the
102 whole year, with a sharp deepening in June and gradual shoaling after July (Figure 3e), reflecting the seasonality
103 of the solar radiation. Unlike the large variability in the depth of the DCM, its magnitude is relatively constant at
104 around 0.62 mg m^{-3} (Figure 3f). In the annually averaged profiles, the observed DCM is located at about 80 m
105 depth with a concentration of 0.52 mg m^{-3} (Figure 4a). The base case succeeds in reproducing the DCM at $65 \pm 7 \text{ m}$
106 depth. However, it fails to reproduce the deepening of the DCM in June and the simulated annually averaged depth
107 of DCM is shallower by about 15 m than the observed. The simulated magnitude of the DCM is about 2-fold larger
108 than the observed (Figure 3f and Figure 4a) and hence the base case generally overestimates vertically integrated
109 chlorophyll (Figure 3b).

110 With respect to phytoplankton and POC, the observed maximum concentration occurs at about 60 m depth,
111 which is 20 m above the DCM (Figure 4b-c). The observed vertical distributions of phytoplankton and POC are
112 not well captured by the base case. For example, phytoplankton and POC in the upper layer are overestimated with
113 the model-data discrepancies exceeding the variability of the observations (Figure 4b-c). As a result, the base case
114 yields an overall overestimation of the vertically integrated phytoplankton and POC (Figure 3c-d).

15 Figure 4b also shows that both observed and simulated phytoplankton approach zero at about 160 m depth.
16 Unlike phytoplankton, the observations show that the POC concentrations are 19 mg C m⁻³ at about 200 m depth
17 because of the existence of detritus, or zooplankton, or both (Figure 4b, c). However, the base case fails to reproduce
18 this non-zero POC concentrations, indicating that the model might be underestimating the carbon export fluxes at
19 200 m.

20 **4.2. Results of the optimizations**

21 **4.2.1. Model-data misfits**

22 The case-specific cost function values and total misfits for the different 1D optimizations are shown in Figure
23 5. Not surprisingly, all optimizations result in a reduction of the case-specific cost function values. The extent of
24 the reductions depends on the specific subset of parameters that were optimized. However, the total misfits are not
25 reduced in all optimizations. Optimizations A1 and A2 lead to slightly larger total misfits than the base case and
26 optimization B2 leads to a significantly larger total misfit. The smallest total cost function values are achieved in
27 A4, B4, and C4, i.e. in the experiments where a larger subset of parameters was optimized (6 parameters). The
28 optimal parameter sets (A4, B2, and C4), which are selected based on case-specific misfit from these three groups,
29 will be used in subsequent analyses and hereafter are denoted simply as experiment A, experiment B, and
30 experiment C. Further comparisons are presented below to assess the impact of the different combinations of
31 observations.

32 **4.2.2. Experiment A: Satellite chlorophyll only**

33 The optimal parameters (Table 2) from experiment A yield a 58% reduction in the misfit for surface
34 chlorophyll (Figure 5d). However, the vertical structure of chlorophyll deteriorates relative to the base case (Figure
35 4a) because of inappropriate estimates of the initial slope ($\alpha=0.0101$; see table 2) and the maximum ratio of
36 chlorophyll to carbon ($\theta_{max}=0.0191$; see table 2). The annually averaged depth of the DCM is lifted up to around
37 30±10m and the magnitude of DCM strongly decreases (Figure 3a, 4b). Similar to chlorophyll, these deteriorations
38 also manifest in the vertical phytoplankton and POC distributions (Figure 4b-c). As a result, experiment A
39 underestimates vertically integrated chlorophyll, phytoplankton, and POC (Fig. 3b-d).

40 4.2.3. Experiment B: Satellite chlorophyll and chlorophyll profiles

41 Due to the addition of observed chlorophyll profiles to the optimization in experiment B, the misfits for surface
42 and subsurface chlorophyll decrease relative to the base case (Figure 5d), but the reduction in the misfit for surface
43 chlorophyll (38%) is smaller than that in experiment A (58%). A straightforward interpretation is that the addition
44 of subsurface observations reduces the model's degrees of freedom to fit one single observation type (surface
45 chlorophyll). The vertical profile of chlorophyll is reproduced better in experiment B than in the base case and
46 experiment A in that the magnitude of the DCM is closer to the observations, although the DCM depth is still too
47 shallow, on average by about 20 m (Figure 4a). The improvement in the vertical chlorophyll structure results in a
48 better model-data fit of vertically integrated chlorophyll (Figure 3b).

49 Despite the improvements in chlorophyll, the vertical profiles of phytoplankton and POC exhibit a marked
50 deterioration relative to the base case and experiment A (Figure 4b-c) because the parameter optimization
51 underestimates the maximum chlorophyll-to-carbon ratio ($\theta_{max}=0.0158$; see table 2). Experiment B leads to an
52 overestimation of phytoplankton and POC relative to the base case with misfits roughly 2.7 and 1.6 times larger
53 than those of the base case, respectively (Figure 5d). Although experiment B reproduces the non-zero POC
54 concentrations at about 200 m depth, the proportion of phytoplankton in the POC pool is incorrect. In contrast to
55 the observations where the phytoplankton's contribution is neglectable (Figure 4), the simulated POC at 200 m is
56 dominated by phytoplankton (49%).

57 4.2.4. Experiment C: All available observations

58 Incorporating all observations (i.e. surface chlorophyll and profiles of chlorophyll, phytoplankton, and POC)
59 in experiment C improves the model-data misfits for almost all aspects except for surface chlorophyll (Figure 3).
60 Although a slight increase in the misfit occurs for the surface chlorophyll (~5%), the total misfit is reduced by 75%
61 compared to the base case. As shown in Figure 4a, the annually averaged depth of DCM of 80 m coincides with
62 the observed DCM, primarily because experiment C reproduces the deepening of the DCM in summer. The
63 magnitude of the DCM is also decreased relative to the base case but remains higher than the observed.
64 Phytoplankton and POC profiles exhibit only minor deviations from the observations (Figure 4b-c). Importantly,
65 experiment C reproduces the non-zero POC concentrations at 200 m. In contrast to experiment B, phytoplankton

66 in experiment C drops to zero at about 160 m and POC is dominated by detritus (85%), which is more consistent
67 with the observations.

68 **4.3. Simulated carbon fluxes**

69 Annually averaged carbon fluxes within the upper 200 m are shown for each experiment in Figure 6. The
70 primary production in the base case amounts to $0.78 \text{ g C m}^{-2} \text{ day}^{-1}$, of which 37% is consumed by zooplankton, and
71 the remaining 63% flows into detritus pools through sloppy feeding, mortality, and aggregation of phytoplankton.
72 As for the production of detritus, contributions from the phytoplankton and zooplankton pools account for 70%
73 and 30%, respectively. Most of the produced detritus is recycled into the nutrient pool fueling recycled primary
74 production, and only a small fraction is removed from the upper layer through gravitational sinking. As a result,
75 carbon export, which is estimated as the sum of sinking fluxes by phytoplankton and detritus, is only 0.00032 g C
76 $\text{m}^{-2} \text{ day}^{-1}$ and accounts for 0.04% of primary production.

77 Due to the underestimation of phytoplankton in experiment A, primary production is reduced to 0.21 g C m^{-2}
78 day^{-1} in that case. All other fluxes in the top 200 m decrease relative to the base case as well, except for the export
79 flux which increases to about 0.8% of primary production. This relative increase in export is the result of larger
80 sinking rates of phytoplankton and detritus ($w_{Phy}=0.95$, $w_{LDet}=4.97$; see table 2) than those used in the base case.

81 In contrast to experiment A, experiment B yields an increase of primary production relative to the base case.
82 The proportion of the grazing flux to primary production and the contribution of zooplankton to the production of
83 detritus also increase to about 59% and 52%, respectively. Unlike in the other three experiments, carbon export in
84 experiment B is dominated by the sinking of phytoplankton, reflecting its large contribution to POC at 200 m.
85 Although the simulated POC concentration at 200 m is very close to the observations, the relative contributions of
86 phytoplankton, zooplankton, and detritus are problematic and likely do not result in a better estimation of carbon
87 export (in this case 0.3% of primary production).

88 In experiment C, primary production is $0.30 \text{ g C m}^{-2} \text{ day}^{-1}$ with 24% flowing to zooplankton. The mortality
89 of zooplankton causes a flux of $0.047 \text{ g C m}^{-2} \text{ day}^{-1}$ to detritus, which accounts for 17% of the production of detritus.
90 Finally, about 24% of primary production is removed from the upper 200 m through gravitational sinking. The
91 simulated export ratio of 24% is within the wide range of reported export ratios, from 6% to 43%, at 120 m depth
92 in the Gulf of Mexico (see Table 3 of Hung et al., 2010). Despite the high degree of uncertainty that exists when

93 estimating export ratios (e.g., the global mean export ratio varies from ~10% (Henson et al., 2012; Lima et al.,
94 2014; Siegel et al., 2014) to ~20% (Henson et al., 2015; Laws et al., 2000)), it is obvious that only experiment C
95 reproduced an export ratio of a reasonable magnitude. A more detailed validation of primary production and export
96 fluxes will be presented in the following sections.

97 **5. 3D biogeochemical model**

98 The optimal parameter sets from the 1D optimizations of A, B, and C were applied in the 3D model for the
99 whole GOM for five years (2011-2015). The performance of the 3D model can be regarded as a cross-validation
00 of the parameters optimized in 1D at different times and locations. It is possible that the optimization algorithm has
01 modified parameters to compensate for biases between 1D and 3D simulations, e.g. the absence of advection in 1D
02 model as well as the differences in the model domain, model period, and model resolution, that degrades the 3D
03 model performance (Kane et al., 2011). Indeed, directly applying the optimal parameter sets from 1D version to
04 the 3D model yields lower model-data agreement than the 1D counterpart but well preserves the most important
05 features. For instance, when the resulting parameters are used in the experiment C, chlorophyll concentrations in
06 the upper layer were lower in the 3D model and farther away from the observations. However, the DCM depth and
07 the non-zero POC concentrations at 200 m with appropriate contributions from each component are well
08 reproduced in the 3D model. We therefore performed a few manual tests and made the following modifications to
09 the optimized parameters to bring the model-data agreement of 3D model in better alignment with that of 1D
10 version (Table 2): the half-saturation for NH_4 uptake (k_{NH_4}) was decreased to 0.01 in experiment B and C, and the
11 aggregation parameter (τ) was decreased to 0.05 in the experiment C.

12 **5.1. Spatial patterns of surface chlorophyll**

13 First, the annual climatological surface chlorophyll from satellite and model are compared from 2011 to 2015.
14 The satellite estimates show high chlorophyll in the coastal regions and low chlorophyll in the deep ocean (Figure
15 7a). This spatial pattern of surface chlorophyll is well reproduced in all simulations except in the experiment A
16 which even fails to reproduce the relatively high chlorophyll near the Mississippi-Atchafalaya river systems
17 because of the high sinking rate of phytoplankton ($w_{\text{Phy}}=0.95$; see Table 2). The largest model-data differences
18 occur in the coastal regions, where all simulations underestimate the observed surface chlorophyll. Since all BGC-
19 Argo floats operated in the deep ocean (Figure 1) and the parameter optimization is performed at one central station

20 without any influence from coastal environments, only the model results in the deep ocean (depth > 1000 m) will
21 be considered in the following discussion.

22 5.2. Subsurface distributions

23 Figure 8 shows the seasonal cycles of surface chlorophyll as well as the vertically integrated chlorophyll,
24 phytoplankton, and POC within the deep ocean (depth>1000 m). Analogous to the 1D models, chlorophyll,
25 phytoplankton, and POC were integrated over the upper 200 m. Here again the whole deep ocean was averaged
26 because it is homogenous horizontally. In addition, we compare surface chlorophyll with satellite estimates in two
27 sub-regions from the Mississippi Delta and the central Gulf in Figure S5.

28 Comparisons of vertical profiles between observations and model results are given in Figure 9. In general,
29 the main features in the 3D models are very similar to those in 1D. Experiment A cannot constrain the vertical
30 profiles of chlorophyll because of the inappropriate estimation of initial slope (α), experiment B overestimates
31 phytoplankton and its contribution to POC since the maximum ratio of chlorophyll to carbon (θ_{max}) is weakly
32 constrained, and experiment C shows significant improvements in the model-data agreement.

33 Additional comparisons of the chlorophyll-to-carbon ratio, primary production, and carbon export fluxes from
34 1D and 3D models with observations are given in Figure 10. The chlorophyll-to-carbon ratio is estimated as the
35 vertically integrated chlorophyll divided by phytoplankton in the upper 200 m (Figure 10a). As an important
36 indicator of phytoplankton physiological status (Geider, 1987), the observed chlorophyll-to-carbon ratio varies
37 considerably in response to the ambient environment. In general, the ratios derived from the 3D models are lower
38 than their corresponding 1D values, but the differences are still within the range of variability. Without utilizing
39 the observations of phytoplankton and POC, experiments A and B in both 1D and 3D versions underestimate the
40 chlorophyll-to-carbon ratio. In experiment C, the simulated chlorophyll-to-carbon ratios from 1D and 3D are in
41 good agreement with the observations although the observed variability is underestimated.

42 For reference, satellite-based primary production (PP) is provided by two algorithms, the Vertically
43 Generalized Production Model (VGPM, Behrenfeld and Falkowski 1997) and the Carbon-based Productivity
44 Model (CbPM, Westberry et al. 2008). As shown in Figure 10b, satellite-based PP differs depending on the
45 algorithm applied. PP results from all 3D simulations which were integrated down to 200 m are qualitatively similar

46 to the 1D simulations. Experiment C provides the best estimates of PP when compared to satellite-based estimates
47 from VGPM and CbPM, both in 1D and 3D.

48 The base case and experiments A and B yield carbon export fluxes smaller by one to two orders of magnitude
49 than experiment C. Thus, only experiment C from the 1D and 3D models are shown in Figure 10c in comparison
50 to observations from sediment traps (see supplementary material). The carbon export fluxes at 200 m from the 1D
51 and 3D are similar in magnitude although the 1D model yields higher fluxes and larger variability. Despite the
52 scarcity of carbon export observations in the GOM, the model estimates are within the range of observations down
53 to ~1,600 m and capture the observed declining trend of carbon export with depth.

54 In summary, all the results above demonstrate the feasibilities of using the locally optimized parameters from
55 the 1D model to improve the 3D simulation. In addition, by incorporating all available observations (i.e. surface
56 chlorophyll from satellite estimates, profiles of chlorophyll, phytoplankton, and POC from bio-optical floats),
57 experiment C can not only simulate the biogeochemical processes well in the upper 200 m, but also reproduce the
58 carbon export flux and its associated attenuation in the deep ocean (200-1600m) of the GOM.

59 **6. Discussion**

60 **6.1. Trade-offs between different observations for parameter optimization**

61 The results of the optimization experiments vary dramatically depending on how many observation types are
62 used. Using only satellite surface chlorophyll in experiment A succeeds in reducing the misfits of surface
63 chlorophyll, but at the expense of the vertical structure since the predominant DCM disappears in experiment A.
64 Satellite surface chlorophyll alone cannot constrain several vital parameters, including the initial slope of the
65 productivity-irradiance curve (α) and the maximum ratio of chlorophyll to carbon (θ_{max}), with confidence. This
66 result highlights the importance of subsurface observations for parameter optimization and similarly for model
67 validation.

68 The floats provide valuable subsurface observations, but chlorophyll profiles alone are not sufficient for
69 parameter optimization. In experiment B, the addition of chlorophyll profiles leads to significant improvements in
70 vertical chlorophyll distributions; however, the profiles of phytoplankton and POC deteriorate largely because the
71 maximum ratio of chlorophyll to carbon (θ_{max}) is poorly constrained. Using estimates of phytoplankton biomass
72 and POC derived from backscatter measurements in experiment C yields the best estimation of plankton-related

73 state variables and carbon fluxes (i.e. primary production and carbon export). Only in this experiment do the
74 improvements obtained from observations in the upper 200 m extend to the deep ocean as reflected in the improved
75 carbon export estimates below 1,000 m.

76 It should be noted, however, that degradation of unoptimized variables did not occur in all optimizations
77 within experiments A and B. In some cases, the unoptimized fields were improved. For example, the A2
78 optimization yields a 69% reduction in the misfit for subsurface chlorophyll (Figure 5d) and large improvements
79 of chlorophyll profiles (Figure S6a) even though no observations of subsurface chlorophyll are used. Another
80 example is that B1 optimization improves simulations of phytoplankton and POC (Figure 5d and Figure S6b-c)
81 through the correlations between the observed chlorophyll and phytoplankton ($R^2 = 0.69$) and POC ($R^2 = 0.69$).
82 Similar findings have been reported in Prunet et al. (1996b) where the improvements of chlorophyll profiles within
83 the mixed layer were obtained by using surface chlorophyll in a 1D model. In a more recent study by Xiao and
84 Friedrichs (2014a) where satellite data was used subsurface fields were improved in addition to surface fields.

85 In optimizations A2 and B1, the improvement in unoptimized fields occurred because the poorly constrained
86 parameters were not optimized but well defined coincidentally ($\alpha = 0.125$ in the optimization A2 and $\theta_{max} = 0.0535$
87 in the optimization B1; see table 2). Including the poorly constrained parameters into the parameter optimization
88 can return a lower misfit with respect to the observations used in optimization but increases the risk of overfitting
89 and reduces the model's predictive skill, i.e. the ability to simulate unoptimized observations and those collected
90 at different locations and times. This is consistent with previous studies (Friedrichs et al., 2006, 2007; Ward et al.,
91 2010). For example, Friedrichs et al. (2006) optimized three ecosystem models of different complexities against
92 three seasons of observations and the resulting parameters were used to quantify the predictive skill for the fourth
93 season. Cross-validation showed that exclusion of the poorly constrained parameters from the optimization
94 increased the predictive skill.

95 Although prior knowledge of the parameters allows one to exclude those poorly constrained ones from the
96 optimization and thus can prevent degradation in unoptimized variables, most parameters are poorly known. Thus,
97 the ultimate resolution of this issue should be to increase availability of observations so that more parameters can
98 be constrained with confidence. In addition, even if the poorly constrained parameters are well-known, a lack of
99 observations hampers our ability to recognize improvements in the model's predictive skill and hence may prevent

00 us from identifying the optimal solutions. For example, without the observations of phytoplankton and POC, we
01 could not have known that optimization B1 improved simulations of phytoplankton and POC, let alone that the
02 optimization B1 was a better solution than the optimization B2 (the experiment B) in terms of the lower total misfit
03 as shown in Figure 5d.

04 It has been suggested that when performing a parameter optimization, not only parameter values but also
05 parameter uncertainties should be taken into account (Fennel et al., 2001; Ward et al., 2010; Bagniewski et al.,
06 2011). The parameter uncertainties can be assessed by performing an uncertainty analysis (Fennel et al., 2001;
07 Prunet et al., 1996a, 1996b), replicating the parameter optimization (Ward et al., 2010), and cross-validating the
08 resulting parameters (Xiao and Friedrichs, 2014a). In this study, a cross-validation of the parameters was conducted
09 by evaluating the model's predictive skill with respect to different variables, times, and locations. However, even
10 when cross-validation at different times and locations produces large misfits, we cannot conclude that the models
11 reproduce observations through wrong mechanisms. This is because the large misfit can be a result of intrinsic
12 heterogeneity of biological parameters at different times (Mattern et al., 2012) and locations (Kidston et al., 2011).
13 Therefore, it is important to evaluate the predictive skill of unoptimized variables.

14 Collectively, the discussion above highlights the values of BGC float data for parameter optimization and
15 model validation, not only because of their high spatio-temporal coverage but also their ability to measure multiple
16 properties simultaneously.

17 **6.2. Feasibilities of applying the local optimized parameters to 3D models**

18 As the high computational cost makes direct optimization for a 3D biogeochemical model impractical, we
19 performed parameter optimizations first in a 1D surrogate model with the same biogeochemical component as the
20 3D model. However, there are some difficulties in porting the locally optimized parameters to the basin-scale
21 model.

22 Firstly, the 1D model necessarily neglects advection and inevitably differs from the 3D model, e.g. in model
23 domain and model resolution. The optimized parameters from the 1D model may have been adjusted to compensate
24 for biases between 1D and 3D models and, as a result, this may degrade the 3D simulations (Kane et al., 2011).
25 Although counter examples also exist where the 3D simulations outperform the 1D models with respect to vertical
26 profiles of phytoplankton and nitrate (Hoshiya et al., 2018), some manual modifications might be necessary before

27 the optimal 1D parameters can be applied in the 3D model. In this study, despite some degradations in 3D
28 simulations, the benefits of the 1D optimization were mostly preserved in the 3D simulations. This greatly
29 simplified the following subjective tuning of the 3D model by limiting the number of parameters that needed to be
30 adjusted and confirmed the feasibility of improving the 3D model by optimizing a 1D surrogate.

31 Secondly, the spatial heterogeneity of parameters (e.g., Kuhn and Fennel 2019) is another issue that influences
32 the portability of parameters from 1D to 3D models. For example, the underestimation of surface chlorophyll in
33 the coastal regions may result from the contrasting ecosystem functioning between coastal regions and deep ocean,
34 whereby the highly productive continental shelf in the northern GOM is fueled by the large nutrient load from the
35 Mississippi and Atchafalaya river systems with primary production being as high as $4 \text{ g C m}^{-2} \text{ day}^{-1}$ near the
36 Mississippi river delta (Fennel et al., 2011), while the deep ocean is oligotrophic and nutrient limited with the
37 primary production ranging from 0.2 to $0.5 \text{ g C m}^{-2} \text{ day}^{-1}$ (see Figure 10). In some studies, the parameter
38 optimization has been performed at several contrasting stations with a goal of using different parameter sets in
39 different regions of the 3D model (Hoshiba et al., 2018). In other studies different stations were optimized
40 simultaneously to obtain one single optimized parameter set (Kane et al., 2011; Oschlies and Schartau, 2005;
41 Schartau and Oschlies, 2003). Such parameters compromise the misfit in each single station but take account into
42 all stations and can often yield an overall better simulation of all these stations as shown by Kuhn and Fennel
43 (2019).

44 7. Conclusions

45 In this study, we have performed parameter optimization for a 1D biogeochemical model and then used the
46 resulting parameters with a few modifications to generate simulations with a corresponding 3D model in the GOM.
47 Three experiments have been conducted by using different combinations of observations (surface chlorophyll from
48 satellite estimates, vertical profiles of chlorophyll, phytoplankton biomass and POC from BGC Argo floats) in
49 order to examine the trade-offs between the different observations for parameter optimization. Two misfit metrics
50 have been defined using the case-specific misfit and the total misfit to measure the models' abilities to reproduce
51 the optimized and unoptimized observations.

52 Model results show that satellite surface chlorophyll alone cannot reproduce well the vertical structures in a
53 biogeochemical model unless profile observations are used in addition. BGC Argo floats are an excellent platform

54 for obtaining such observations at high spatio-temporal coverage and for a relatively broad suite of parameters.
55 Only adding chlorophyll profiles is not sufficient because they fail to constrain the ratio of chlorophyll to
56 phytoplankton, but the addition of backscatter, which allows estimation of phytoplankton biomass and POC,
57 enables us to constrain the subsurface carbon state variables and reproduce well PP and carbon export fluxes to
58 below 1000 m depth. Finally, our 3D model was improved and reproduced similar results as the 1D version, which
59 is promising for the application of parameter optimization.

60

61 *Code and data availability:* The ROMS model code can be accessed at <http://www.myroms.com> (last access: 16
62 June 2016). HYCOM data can be downloaded at <http://tds.hycom.org/thredds/dodsC/datasets> (last access: 16
63 August 2018). Profiling data from the BGC-Argo floats are available at the National Oceanographic Data Center
64 (NOAA), <https://data.nodc.noaa.gov/cgi-bin/iso?id=gov.noaa.nodc:159562> (Hamilton and Leidos, 2017)

65

66 *Author contributions.* BW and KF conceived the study. BW carried out optimization experiments, model
67 simulations and analyses. LY assisted with set-up and validation of the 3D model. CG assisted with processing of
68 the BGC float data. BW and KF discussed the results and wrote the paper with contributions from the coauthors.

69

70 *Competing interests.* The authors declare that they have no conflict of interest.

71

72 *Financial support.* This research was funded by the Gulf of Mexico Research Initiative (GoMRI-V-487).

73

74

75

76

77

78

79

81 **References**

- 82 Bagniewski, W., Fennel, K., Perry, M. J. and D'Asaro, E. A.: Optimizing models of the North Atlantic spring
83 bloom using physical, chemical and bio-optical observations from a Lagrangian float, *Biogeosciences*, 8,
84 1291–1307, doi:10.5194/bg-8-1291-2011, 2011.
- 85 Behrenfeld, M. J. and Falkowski, P. G.: Photosynthetic rates derived from satellite-based chlorophyll
86 concentration, *Limnology and Oceanography*, 42(1), 1–20, 1997.
- 87 Behrenfeld, M. J., Boss, E., Siegel, D. A. and Shea, D. M.: Carbon-based ocean productivity and phytoplankton
88 physiology from space, *Global Biogeochemical Cycles*, 19(1), 1–14, doi:10.1029/2004GB002299, 2005.
- 89 Biogeochemical-Argo Planning Group: The scientific rationale, design and implementation plan for a
90 Biogeochemical-Argo float array, edited by Ken Johnson and Hervé Claustre., 2016.
- 91 Boss, E. B. and Haëntjens, N.: Primer regarding measurements of chlorophyll fluorescence and the backscattering
92 coefficient with WETLabs FLBB on profiling floats., 2016.
- 93 Briggs, N., Perry, M. J., Cetinic', I., Lee, C., D'Asaro, E., Gray, A. M. and Rehm, E.: High-resolution observations
94 of aggregate flux during a sub-polar North Atlantic spring bloom, *Deep-Sea Research I*, 58, 1031–1039,
95 doi:10.1016/j.dsr.2011.07.007, 2011.
- 96 Cullen, J. J.: Subsurface Chlorophyll Maximum Layers : Enduring Enigma or Mystery Solved ?, *Annual Review*
97 *of Marine Science*, 7, 207–239, doi:10.1146/annurev-marine-010213-135111, 2015.
- 98 Denman, K. L.: Modelling planktonic ecosystems : parameterizing complexity, *Progress in Oceanography*, 57,
99 429–452, doi:10.1016/S0079-6611(03)00109-5, 2003.
- 00 Doney, S. C., Lima, I., Moore, J. K., Lindsay, K., Behrenfeld, M. J., Westberry, T. K., Mahowald, N., Glover, D.
01 M. and Takahashi, T.: Skill metrics for confronting global upper ocean ecosystem-biogeochemistry models
02 against field and remote sensing data, *Journal of Marine Systems*, 76, 95–112,
03 doi:10.1016/j.jmarsys.2008.05.015, 2009.
- 04 Fennel, K. and Boss, E.: Subsurface maxima of phytoplankton and chlorophyll : Steady-state solutions from a
05 simple model, *Limnology and Oceanography*, 48(4), 1521–1534, 2003.
- 06 Fennel, K., Losch, M., Schroter, J. and Wenzel, M.: Testing a marine ecosystem model : sensitivity analysis and

07 parameter optimization, *Journal of Marine Systems*, 28, 45–63, 2001.

08 Fennel, K., Wilkin, J., Levin, J., Moisan, J., Reilly, J. O. and Haidvogel, D.: Nitrogen cycling in the Middle Atlantic
09 Bight: Results from a three-dimensional model and implications for the North Atlantic nitrogen budget,
10 *GLOBAL BIOGEOCHEMICAL CYCLES*, 20, 1–14, doi:10.1029/2005GB002456, 2006.

11 Fennel, K., Hetland, R., Feng, Y. and Dimarco, S.: A coupled physical-biological model of the Northern Gulf of
12 Mexico shelf: Model description, validation and analysis of phytoplankton variability, *Biogeosciences*, 8,
13 1881–1899, doi:10.5194/bg-8-1881-2011, 2011.

14 Fommervault, O. P. De, Perez-brunius, P., Damien, P., Camacho-ibar, V. F. and Sheinbaum, J.: Temporal
15 variability of chlorophyll distribution in the Gulf of Mexico: bio-optical data from profiling floats,
16 *Biogeosciences*, 14, 5647–5662, doi:10.5194/bg-14-5647-2017, 2017.

17 Friedrichs, M. A. M., Hood, R. R. and Wiggert, J. D.: Ecosystem model complexity versus physical forcing:
18 Quantification of their relative impact with assimilated Arabian Sea data, *Deep-Sea Research Part II*, 53, 576–
19 600, doi:10.1016/j.dsr2.2006.01.026, 2006.

20 Friedrichs, M. A. M., Dusenberry, J. A., Anderson, L. A., Armstrong, R. A., Chai, F., Christian, J. R., Doney, S.
21 C., Dunne, J., Fujii, M., Hood, R., Jr, D. J. M., Moore, J. K., Schartau, M., Spitz, Y. H. and Wiggert, J. D.:
22 Assessment of skill and portability in regional marine biogeochemical models: Role of multiple planktonic
23 groups, *Journal of Geophysical Research*, 112, 1–22, doi:10.1029/2006JC003852, 2007.

24 Geider, R. J.: Light and temperature dependence of the carbon to chlorophyll a ratio in microalgae and
25 cyanobacteria: implications for physiology and growth of phytoplankton, *New Phytologist*, 106, 1–34, 1987.

26 Geider, R. J., MacIntyre, H. L. and Kana, T. M.: Dynamic model of phytoplankton growth and acclimation :
27 responses of the balanced growth rate and the chlorophyll a : carbon ratio to light , nutrient-limitation and
28 temperature, *Marine ecology progress series*, 148, 187–200, 1997.

29 Gomez, F. A., Lee, S., Liu, Y., Jr, F. J. H., Muller-karger, F. E. and Lanmkin, J. T.: Seasonal patterns in
30 phytoplankton biomass across the northern and deep Gulf of Mexico : a numerical model study,
31 *Biogeosciencesg*, 15, 3561–3576, doi:10.5194/bg-15-3561-2018, 2018.

32 Green, R. E., Bower, A. S. and Lugo-Fernandez, A.: First Autonomous Bio-Optical Profiling Float in the Gulf of
33 Mexico Reveals Dynamic Biogeochemistry in Deep Waters, *PLoS ONE*, 9(7), 1–9,

34 doi:10.1371/journal.pone.0101658, 2014.

35 Haidvogel, D. B., Arango, H., Budgell, W. P., Cornuelle, B. D., Curchitser, E., Lorenzo, E. Di, Fennel, K., Geyer,
36 W. R., Hermann, A. J., Lanerolle, L., Levin, J., McWilliams, J. C., Miller, A. J., Moore, A. M., Powell, T. M.,
37 Shchepetkin, A. F., Sherwood, C. R., Signell, R. P., Warner, J. C. and Wilkin, J.: Ocean forecasting in terrain-
38 following coordinates : Formulation and skill assessment of the Regional Ocean Modeling System, *Journal of*
39 *computational physics*, 227, 3595–3624, doi:10.1016/j.jcp.2007.06.016, 2008.

40 Hamilton, P. and Leidos: Ocean currents, temperatures, and others measured by drifters and profiling floats for the
41 Lagrangian Approach to Study the Gulf of Mexico Deep Circulation project 2011-07 to 2015-06 (NCEI
42 Accession 0159562), Version 1.1, NOAA National Centers for Environmental Information. Dataset, available
43 at <https://accession.nodc.noaa.gov/0159562>, last access: 25 October 2017.

44 Henson, S. A., Sanders, R. and Madsen, E.: Global patterns in efficiency of particulate organic carbon export and
45 transfer to the deep ocean, *Global Biogeochemical Cycles*, 26(1), doi:10.1029/2011GB004099, 2012.

46 Henson, S. A., Yool, A. and Sanders, R.: Variability in efficiency of particulate organic carbon export: A model
47 study, *Global Biogeochemical Cycles*, 29(1), 33–45, doi:10.1002/2014GB004965, 2015.

48 Hoshiba, Y., Hirata, T., Shigemitsu, M., Nakano, H., Hashioka, T., Masuda, Y. and Yamanaka, Y.: Biological data
49 assimilation for parameter estimation of a phytoplankton functional type model for the western North Pacific,
50 *Ocean Science*, 14, 371–386, doi:10.5194/os-14-371-2018, 2018.

51 Hung, C.-C., Xu, C., Santschi, P. H., Zhang, S.-J., Schwehr, K. A., Quigg, A., Guo, L., Gong, G.-C., Pinckney, J.
52 L., Long, R. A. and Wei, C.-L.: Comparative evaluation of sediment trap and ²³⁴Th-derived POC fluxes from
53 the upper oligotrophic waters of the Gulf of Mexico and the subtropical northwestern Pacific Ocean, *Marine*
54 *Chemistry*, 121(1), 132–144, doi:<https://doi.org/10.1016/j.marchem.2010.03.011>, 2010.

55 Kane, A., Moulin, C., Thiria, S., Bopp, L., Berrada, M., Tagliabue, A., Crépon, M., Aumont, O. and Badran, F.:
56 Improving the parameters of a global ocean biogeochemical model via variational assimilation of in situ data
57 at five time series stations, *Journal of Geophysical Research: Oceans*, 116, 1–14, doi:10.1029/2009JC006005,
58 2011.

59 Kidston, M., Matear, R. and Baird, M. E.: Parameter optimisation of a marine ecosystem model at two contrasting
60 stations in the Sub-Antarctic Zone, *Deep-Sea Research II*, 58, 2301–2315, doi:10.1016/j.dsr2.2011.05.018,

61 2011.

62 Kuhn, A. M. and Fennel, K.: Evaluating ecosystem model complexity for the northwest North Atlantic through
63 surrogate-based optimization, *Ocean Modelling*, 142, 101437,
64 doi:<https://doi.org/10.1016/j.ocemod.2019.101437>, 2019.

65 Kuhn, A. M., Fennel, K. and Mattern, J. P.: Progress in Oceanography Model investigations of the North Atlantic
66 spring bloom initiation, *Progress in Oceanography*, 138, 176–193, doi:10.1016/j.pocean.2015.07.004, 2015.

67 Kuhn, A. M., Fennel, K. and Berman-frank, I.: Modelling the biogeochemical effects of heterotrophic and
68 autotrophic N₂ fixation in the Gulf of Aqaba (Israel), Red Sea, *Biogeosciences*, 15, 7379–7401,
69 doi:10.5194/bg-15-7379-2018, 2018.

70 Lagman, K. B., Fennel, K., Thompson, K. R. and Bianucci, L.: Assessing the utility of frequency dependent
71 nudging for reducing biases in biogeochemical models, *Ocean Modelling*, 81, 25–35,
72 doi:<https://doi.org/10.1016/j.ocemod.2014.06.006>, 2014.

73 Laurent, A., Fennel, K., Cai, W. J., Huang, W. J., Barbero, L. and Wanninkhof, R.: Eutrophication-induced
74 acidification of coastal waters in the northern Gulf of Mexico: Insights into origin and processes from a
75 coupled physical-biogeochemical model, *Geophysical Research Letters*, 44(2), 946–956,
76 doi:10.1002/2016GL071881, 2017.

77 Laws, E. A., Falkowski, P. G., Smith Jr., W. O., Ducklow, H. and McCarthy, J. J.: Temperature effects on export
78 production in the open ocean, *Global Biogeochemical Cycles*, 14(4), 1231–1246,
79 doi:10.1029/1999GB001229, 2000.

80 Lehmann, M. K., Fennel, K. and He, R.: Statistical validation of a 3-D bio-physical model of the western North
81 Atlantic, *Biogeosciences*, 6(10), 1961–1974, doi:10.5194/bg-6-1961-2009, 2009.

82 Lima, I. D., Lam, P. J. and Doney, S. C.: Dynamics of particulate organic carbon flux in a global ocean model,
83 *Biogeosciences*, 11(4), 1177–1198, doi:10.5194/bg-11-1177-2014, 2014.

84 Martínez-López, B. and Zavala-Hidalgo, J.: Seasonal and interannual variability of cross-shelf transports of
85 chlorophyll in the Gulf of Mexico, *Journal of Marine Systems*, 77, 1–20, doi:10.1016/j.jmarsys.2008.10.002,
86 2009.

87 Martinez-Vicente, V., Dall’Olmo, G., Tarran, G., Boss, E. and Sathyendranath, S.: Optical backscattering is

88 correlated with phytoplankton carbon across the Atlantic Ocean, *Geophysical Research Letters*, 40, 1154–
89 1158, doi:10.1002/grl.50252, 2013.

90 Matear, R. J.: Parameter optimization and analysis of ecosystem models using simulated annealing : A case study
91 at Station P, *Journal of Marine Research*, 53, 571–607, 1995.

92 Mattern, J. P. and Edwards, C. A.: Simple parameter estimation for complex models — Testing evolutionary
93 techniques on 3-dimensional biogeochemical ocean models, *Journal of Marine Systems*, 165, 139–152,
94 doi:10.1016/j.jmarsys.2016.10.012, 2017.

95 Mattern, J. P., Fennel, K. and Dowd, M.: Estimating time-dependent parameters for a biological ocean model using
96 an emulator approach, *Journal of Marine Systems*, 96–97, 32–47,
97 doi:https://doi.org/10.1016/j.jmarsys.2012.01.015, 2012.

98 Mellor, G. L. and Yamada, T.: Development of a turbulence closure model for geophysical fluid problems, *Reviews*
99 *of Geophysics and Space Physics*, 20(4), 851–875, doi:10.1029/RG020i004p00851, 1982.

00 Mignot, A., Claustre, H., Uitz, J., Poteau, A., D’Ortenzio, F. and Xing, X.: Understanding the seasonal dynamics
01 of phytoplankton biomass and the deep chlorophyll maximum in oligotrophic environments: A Bio-Argo float
02 investigation, *Global Biogeochemical Cycles*, 28(8), 1–21, doi:10.1002/2013GB004781, 2014.

03 Muller-Karger, F. E., Walsh, J. J., Evans, R. H. and Meyers, M. B.: On the Seasonal Phytoplankton Concentration
04 and Sea Surface Temperature Cycles of the Gulf of Mexico as Determined by Satellites, *Journal of*
05 *Geophysical Research*, 96, 12645–12665, 1991.

06 Muller-Karger, F. E., Smith, J. P., Werner, S., Chen, R., Roffer, M., Liu, Y., Muhling, B., Lindo-atichati, D.,
07 Lamkin, J., Cerdeira-estrada, S. and Enfield, D. B.: Natural variability of surface oceanographic conditions in
08 the offshore Gulf of Mexico, *Progress in Oceanography*, 134, 54–76, doi:10.1016/j.pocean.2014.12.007, 2015.

09 Oschlies, A. and Schartau, M.: Basin-scale performance of a locally optimized marine ecosystem model, *Journal*
10 *of Marine Research*, 63(2), 335–358, 2005.

11 Prunet, P., Minster, J., Ruiz-Pino, D. and Dadou, I.: Assimilation of surface data in a one-dimensional physical-
12 biogeochemical model of the surface ocean 1 . Method and preliminary results, *GLOBAL*
13 *BIOGEOCHEMICAL CYCLES*, 10(1), 111–138, 1996a.

14 Prunet, P., Minster, J., Echevin, V. and Dadou, I.: Assimilation of surface data in a one-dimensional physical-

15 biogeochemical model of the surface ocean 2. Adjusting a simple trophic model to chlorophyll, temperature,
16 nitrate, and pCO₂ data, *GLOBAL BIOGEOCHEMICAL CYCLES*, 10(1), 139–158, 1996b.

17 Rasse, R., Dall’Olmo, G., Graff, J., Westberry, T. K., van Dongen-Vogels, V. and Behrenfeld, M. J.: Evaluating
18 Optical Proxies of Particulate Organic Carbon across the Surface Atlantic Ocean, *Frontiers in Marine Science*,
19 4(November), 1–18, doi:10.3389/fmars.2017.00367, 2017.

20 Roemmich, D., Alford, M. H., Claustre, H., Johnson, K., King, B., Moum, J., Oke, P., Owens, W. B., Pouliquen,
21 S., Purkey, S., Scanderbeg, M., Suga, T., Wijffels, S., Zilberman, N., Bakker, D., Baringer, M., Belbeoch, M.,
22 Bittig, H. C., Boss, E., Calil, P., Carse, F., Carval, T., Chai, F., Conchubhair, D. Ó., D’Ortenzio, F., Dall’Olmo,
23 G., Desbruyeres, D., Fennel, K., Fer, I., Ferrari, R., Forget, G., Freeland, H., Fujiki, T., Gehlen, M., Greenan,
24 B., Hallberg, R., Hibiya, T., Hosoda, S., Jayne, S., Jochum, M., Johnson, G. C., Kang, K., Kolodziejczyk, N.,
25 Körtzinger, A., Traon, P.-Y. Le, Lenn, Y.-D., Maze, G., Mork, K. A., Morris, T., Nagai, T., Nash, J., Garabato,
26 A. N., Olsen, A., Pattabhi, R. R., Prakash, S., Riser, S., Schmechtig, C., Schmid, C., Shroyer, E., Sterl, A.,
27 Sutton, P., Talley, L., Tanhua, T., Thierry, V., Thomalla, S., Toole, J., Troisi, A., Trull, T. W., Turton, J.,
28 Velez-Belchi, P. J., Walczowski, W., Wang, H., Wanninkhof, R., Waterhouse, A. F., Waterman, S., Watson,
29 A., Wilson, C., Wong, A. P. S., Xu, J. and Yasuda, I.: On the Future of Argo: A Global, Full-Depth, Multi-
30 Disciplinary Array, *Frontiers in Marine Science*, 6, 439 [online] Available from:
31 <https://www.frontiersin.org/article/10.3389/fmars.2019.00439>, 2019.

32 Schartau, M. and Oschlies, A.: Simultaneous data-based optimization of a 1D-ecosystem model at three locations
33 in the North Atlantic : Part I — Method and parameter estimates, *Journal of Marine Research*, 61, 765–793,
34 2003.

35 Shchepetkin, A. F. and McWilliams, J. C.: The regional oceanic modeling system (ROMS): a split-explicit, free-
36 surface, topography-following-coordinate oceanic model, *Ocean Modelling*, 9, 347–404,
37 doi:10.1016/j.ocemod.2004.08.002, 2005.

38 Siegel, D. A., Buesseler, K. O., Doney, S. C., Salliey, S. F., Behrenfeld, M. J. and Boyd, P. W.: Global assessment
39 of ocean carbon export by combining satellite observations and food-web models, *Global Biogeochemical*
40 *Cycles*, 28(3), 181–196, doi:10.1002/2013GB004743, 2014.

41 Smagorinsky, J.: General circulation experiments with the primitive equations: I. the basic experiment, *Monthly*

42 Weather Review, 91(3), 99–164, 1963.

43 Smolarkiewicz, P. K. and Margolin, L. G.: MPDATA : A Finite-Difference Solver for Geophysical Flows, Journal
44 of computational physics, 140, 459–480, 1998.

45 Tjiputra, J. F., Polzin, D. and Winguth, A. M. E.: Assimilation of seasonal chlorophyll and nutrient data into an
46 adjoint three-dimensional ocean carbon cycle model: Sensitivity analysis and ecosystem parameter
47 optimization, Global Biogeochemical Cycles, 21, 1–13, doi:10.1029/2006GB002745, 2007.

48 Ward, B. A., Friedrichs, M. A. M., Anderson, T. R. and Oschlies, A.: Parameter optimisation techniques and the
49 problem of underdetermination in marine biogeochemical models, Journal of Marine Systems, 81, 34–43,
50 doi:10.1016/j.jmarsys.2009.12.005, 2010.

51 Westberry, T., Behrenfeld, M. J., Siegel, D. A. and Boss, E.: Carbon-based primary productivity modeling with
52 vertically resolved photoacclimation, GLOBAL BIOGEOCHEMICAL CYCLES, 22, 1–18,
53 doi:10.1029/2007GB003078, 2008.

54 Xiao, Y. and Friedrichs, M. A. M.: The assimilation of satellite-derived data into a one-dimensional lower trophic
55 level marine ecosystem model, Journal of Geophysical Research: Oceans, 119, 2691–2712,
56 doi:10.1002/2013JC009433.Received, 2014a.

57 Xiao, Y. and Friedrichs, M. A. M.: Using biogeochemical data assimilation to assess the relative skill of multiple
58 ecosystem models in the Mid-Atlantic Bight : effects of increasing the complexity of the planktonic food web,
59 Biogeosciences, 11, 3015–3030, doi:10.5194/bg-11-3015-2014, 2014b.

60 Xue, Z., He, R., Fennel, K., Cai, W., Lohrenz, S. and Hopkinson, C.: Modeling ocean circulation and
61 biogeochemical variability in the Gulf of Mexico, Biogeosciences, 10, 7219–7234, doi:10.5194/bg-10-7219-
62 2013, 2013.

63 Yu, L., Fennel, K. and Laurent, A.: A modeling study of physical controls on hypoxia generation in the northern
64 Gulf of Mexico, Journal of Geophysical Research: Oceans, 120(7), 5019–5039, doi:10.1002/2014JC010634,
65 2015.

66
67
68

69
70
71
72
73
74
75
76
77
78
79

80 **Table list**

81 Table 1. Initial values and ranges of primary parameters used in the biogeochemical model

| Descriptions (unit) | Symbol | Value | Range |
|---|-------------------|---------------------|---------------------------------------|
| Radiation threshold for nitrification (W m^{-2}) | I_0 | 0.0095 ^a | 0.005 ^b -0.01 ^b |
| Half-saturation radiation for nitrification (W m^{-2}) | k_I | 0.1 ^a | 0.01 ^b -0.5 ^b |
| Maximum nitrification rate (day^{-1}) | n_{max} | 0.2 ^c | 0.01 ^b -0.35 ^b |
| Phytoplankton growth at 0 °C (Dimensionless) | μ_0 | 0.69 ^a | 0.1 ^b -3.0 ^b |
| Initial slope of P-I curve ($\text{mg}_C (\text{mg}_C \text{hl W m}^{-2} \text{day})^{-1}$) | α | 0.125 ^a | 0.007 ^a -0.13 ^a |
| Half-saturation for NO_3 uptake ($\text{mmol}_N \text{m}^{-3}$) | k_{NO_3} | 0.5 ^a | 0.007 ^a -1.5 ^a |
| Half-saturation for NH_4 uptake ($\text{mmol}_N \text{m}^{-3}$) | k_{NH_4} | 0.5 ^a | 0.007 ^a -1.5 ^a |
| Phytoplankton mortality (day^{-1}) | m_P | 0.075 | 0.01 ^b -0.2 ^b |
| Aggregation parameter (day^{-1}) | τ | 0.1 | 0.01 ^b -25 ^b |
| Maximum chlorophyll to carbon ratio ($\text{mg}_C \text{hl mg}_C^{-1}$) | θ_{max} | 0.0535 ^c | 0.005 ^a -0.15 ^b |
| Phytoplankton sinking velocity (m day^{-1}) | w_{Phy} | 0.1 ^a | 0.009 ^a -25 ^a |
| Maximum grazing rate (day^{-1}) | g_{max} | 0.6 ^a | 0.1 ^b -4 ^b |

| | | | |
|---|------------|-------------------|---------------------------------------|
| Half-saturation for phytoplankton ingestion ((mmol_N m ⁻³) ²) | k_P | 0.5 | 0.01 ^b -3.5 ^a |
| Zooplankton assimilation efficiency (Dimensionless) | β | 0.75 ^a | 0.25 ^b -0.75 ^b |
| Zooplankton basal metabolism (day ⁻¹) | l_{BM} | 0.01 | 0.01 ^b -0.15 ^b |
| Zooplankton specific excretion (day ⁻¹) | l_E | 0.1 ^a | 0.05 ^b -0.35 ^b |
| Zooplankton mortality (day ⁻¹) | m_Z | 0.2 | 0.02 ^b -0.35 ^b |
| Small detritus remineralization (day ⁻¹) | r_{SD} | 0.3 ^c | 0.005 ^b -0.25 ^a |
| Large detritus remineralization (day ⁻¹) | r_{LD} | 0.1 | 0.005 ^b -0.25 ^a |
| Small detritus sinking velocity (m day ⁻¹) | w_{SDet} | 0.1 ^a | 0.009 ^a -25 ^a |
| Large detritus sinking velocity (m day ⁻¹) | w_{LDet} | 1 ^a | 0.009 ^a -25 ^a |

82 a Fennel et al. (2006); b Kuhn et al. (2018); c Yu et al. (2015)

83

84

85 Table 2. The best fit of parameter set for each optimization experiment. **Dashed lines represent these parameters**
86 **are not included in the parameter optimization and use their prior values. The optimal optimization A4, B2, and C4**
87 **which are further discussed and are denoted simply as experiment A, B, and C are highlighted as bold.**

| | | w_{Phy} | m_P | k_{NH4} | τ | θ_{max} | α | w_{LDet} |
|----------|-----------|---------------|---------------|---------------|--------|----------------|---------------|---------------|
| | Base | 0.1000 | 0.0750 | 0.5000 | 0.1000 | 0.0535 | 0.1250 | 1.000 |
| 1D model | A1 | 0.0608 | 0.0100 | 1.5000 | -- | -- | -- | -- |
| | A2 | 0.6863 | 0.0100 | 0.0195 | -- | 0.0169 | -- | -- |
| | A3 | 1.6567 | 0.1978 | 0.1004 | -- | 0.0250 | 0.0219 | -- |
| | A4 | 0.9468 | 0.0737 | 0.2454 | -- | 0.0191 | 0.0101 | 4.9694 |
| 3D model | A | 0.9468 | 0.0737 | 0.0100 | -- | 0.0191 | 0.0101 | 4.9694 |
| 1D model | B1 | 0.2863 | 0.0983 | 1.5000 | -- | -- | -- | -- |
| | B2 | 0.4217 | 0.0130 | 0.0300 | -- | 0.0158 | -- | -- |
| | B3 | 2.1016 | 0.0176 | 1.5000 | -- | 0.0346 | 0.0079 | -- |
| | B4 | 0.0090 | 0.0100 | 1.5000 | -- | 0.0361 | 0.0405 | 8.3514 |
| 3D model | B | 0.4217 | 0.0130 | 0.0100 | -- | 0.0158 | -- | -- |

| | | w_{Phy} | r_{LD} | m_P | τ | k_{NH_4} | w_{LDet} | θ_{max} |
|----------|-----------|---------------|---------------|---------------|---------------|---------------|---------------|----------------|
| | Base | 0.1000 | 0.1000 | 0.0750 | 0.1000 | 0.5000 | 1.0000 | 0.0535 |
| 1D model | C1 | 1.9231 | 0.2500 | 0.1805 | -- | -- | -- | -- |
| | C2 | 0.9755 | 0.2500 | 0.0100 | 1.1402 | -- | -- | -- |
| | C3 | 0.4071 | 0.0630 | 0.0100 | 1.8531 | 0.0070 | -- | -- |
| | C4 | 0.0090 | 0.0050 | 0.0634 | 0.0995 | 0.0431 | 5.6623 | -- |
| | C5 | 0.0090 | 0.2245 | 0.0100 | 0.6451 | 1.5000 | 2.5202 | 0.0614 |
| 3D model | C | 0.0090 | 0.0050 | 0.0634 | 0.0500 | 0.0100 | 5.6623 | -- |

88

89

90

91

92

93

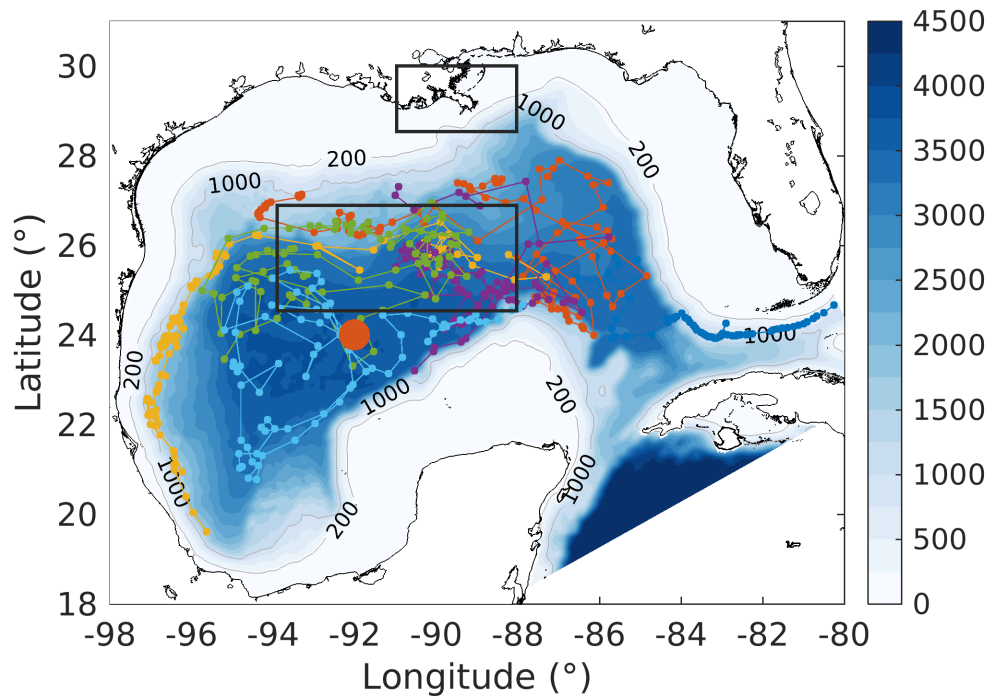
94

95

96

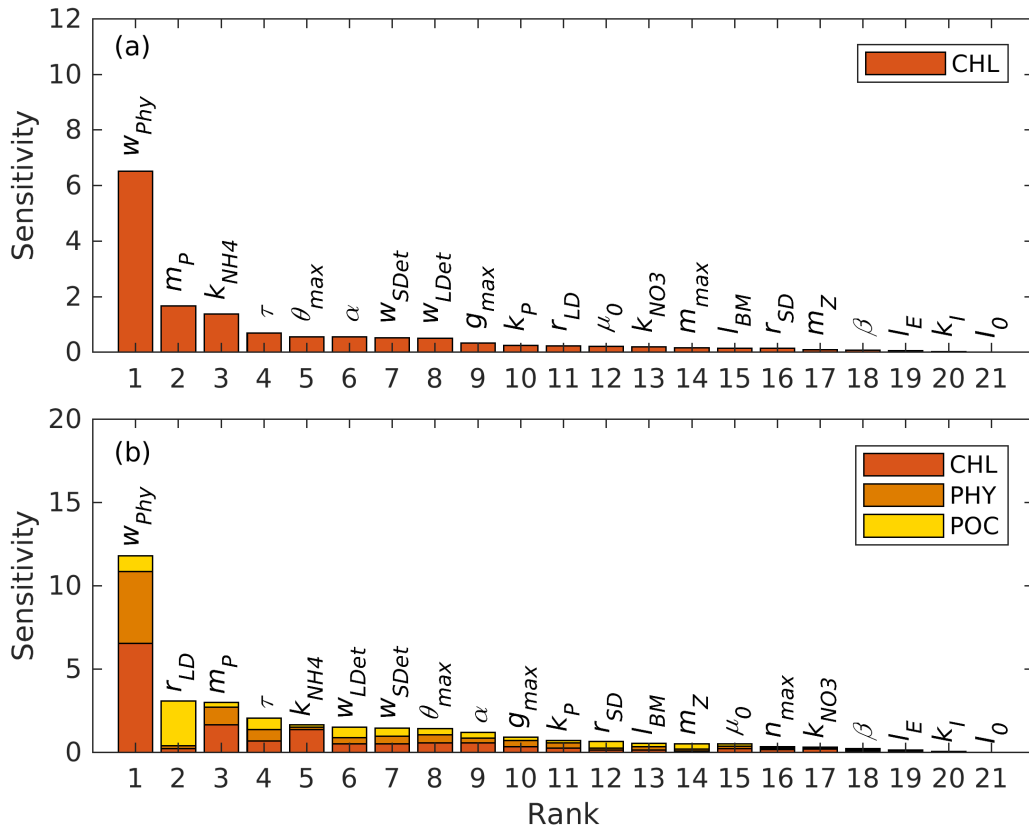
97 **Figure captions**

98



99

00 Figure 1. Model bathymetry (unit: m) with trajectories of six bio-optical floats (small colored dots and lines) which
 01 were operated in the Gulf of Mexico from 2011 to 2015. The location of the 1D model is denoted by the large
 02 orange dot. The north and south black boxes represent the Mississippi Delta and the central gulf, respectively to
 03 show comparisons of surface chlorophyll in Figure S5.

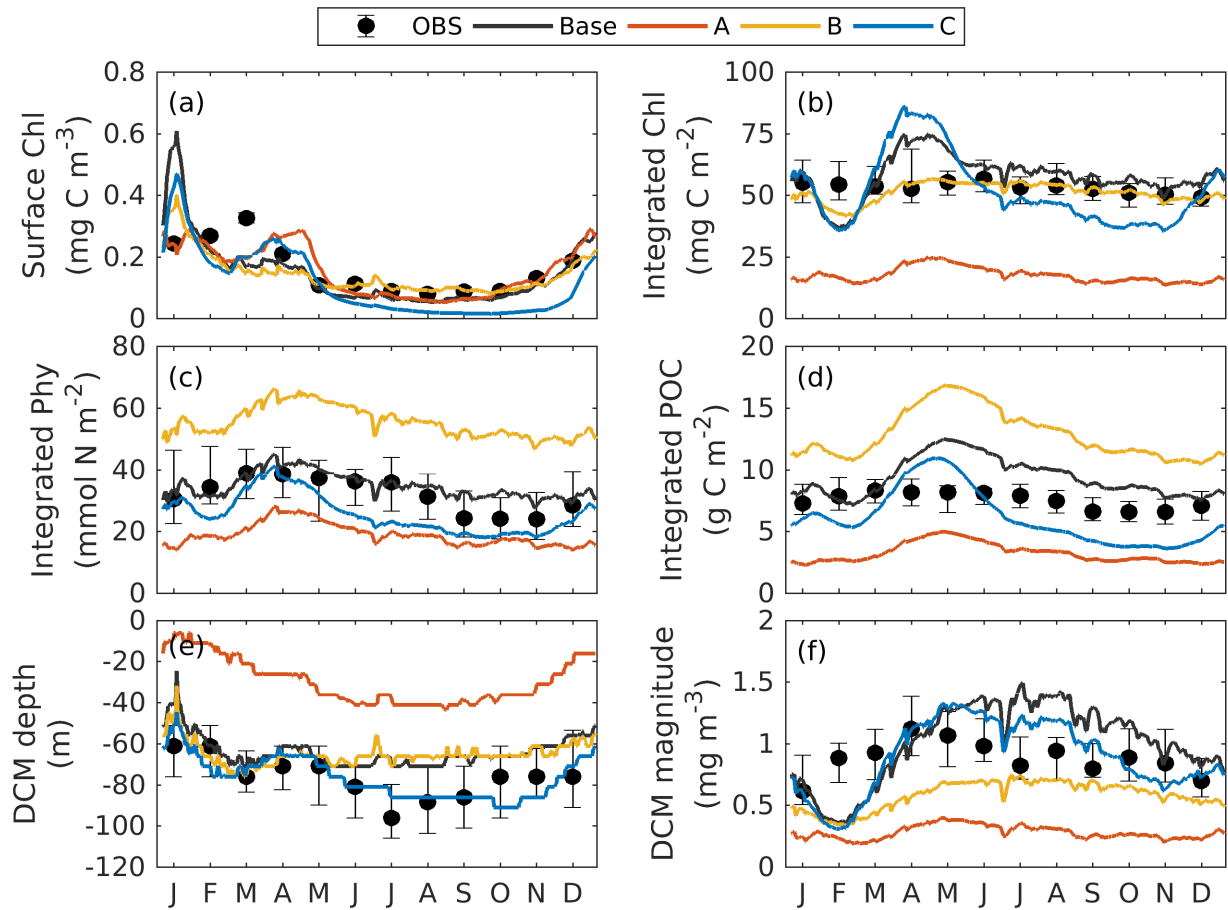


04

05 Figure 2. Parameter sensitivities (unit: dimensionless) with respect to (a) chlorophyll and (b) the sum of
 06 chlorophyll, phytoplankton, and POC.

07

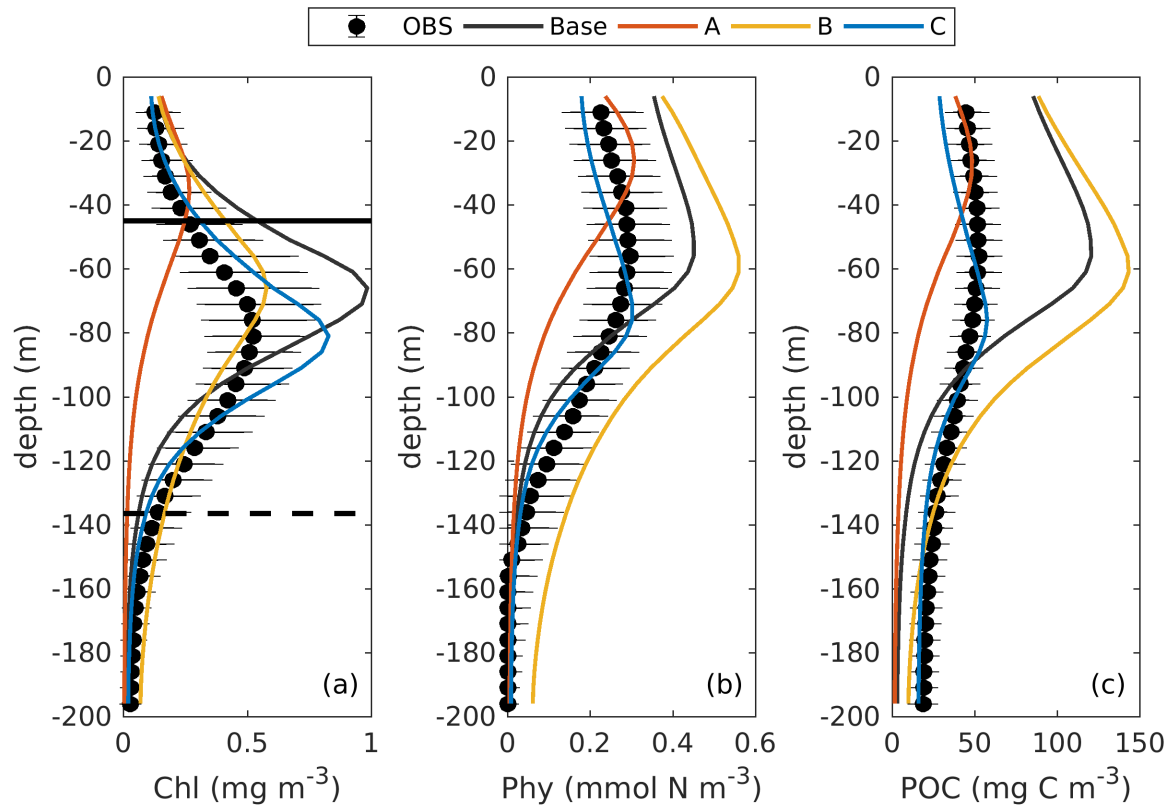
08



09

10 Figure 3. Annual cycle of surface chlorophyll (a), vertically integrated chlorophyll (b), vertically integrated
 11 phytoplankton (c), vertically integrated POC (d), and the depth (e) and magnitude (f) of the DCM from observations
 12 (black dots with error bars), the Base case (black lines), the experiment A (orange lines; only satellite surface
 13 chlorophyll is used), B (yellow lines; satellite surface chlorophyll and float profiles of chlorophyll are used), and
 14 C (blue lines; all available observations are used). Chlorophyll, phytoplankton, and POC are integrated over the
 15 top 200 m. Black error bars represent the interquartile range of observations.

16



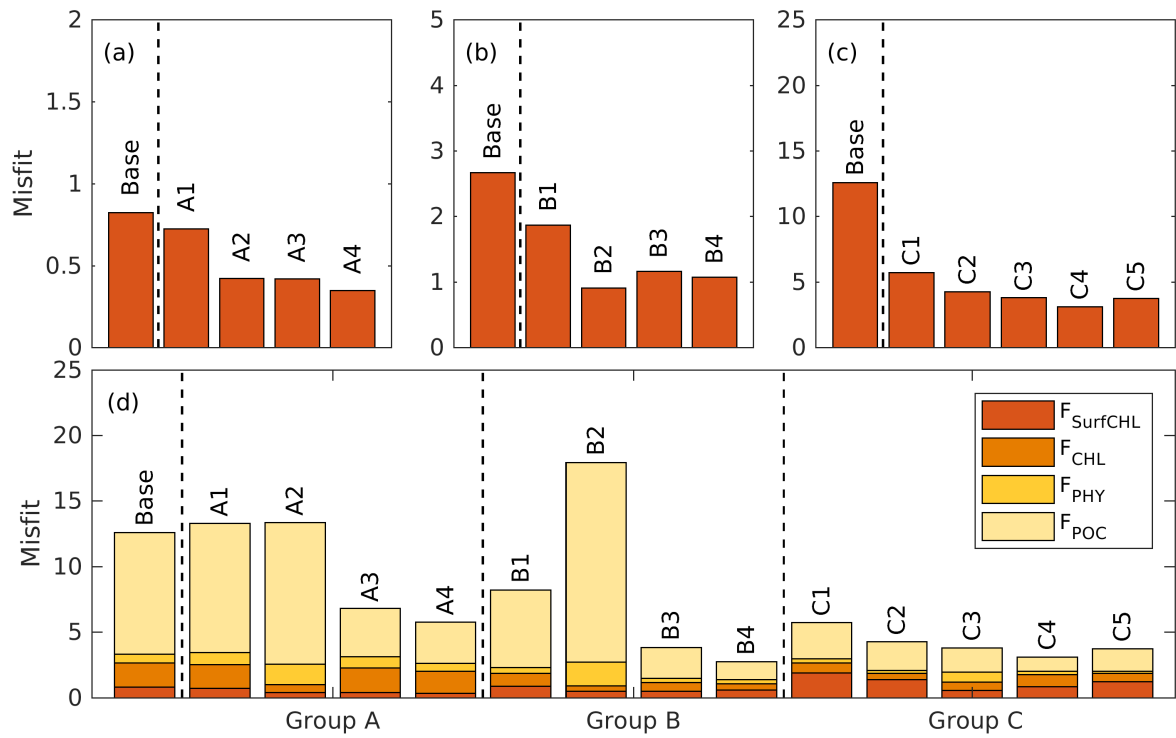
17

18

19

20

Figure 4. Observed (black dots with error bars) and simulated (colored lines) vertical profiles of chlorophyll, phytoplankton, and POC. Black errors represent the interquartile range of observations. The solid and dashed black lines in panel a represent the median values of mixed layer depth from July and December.



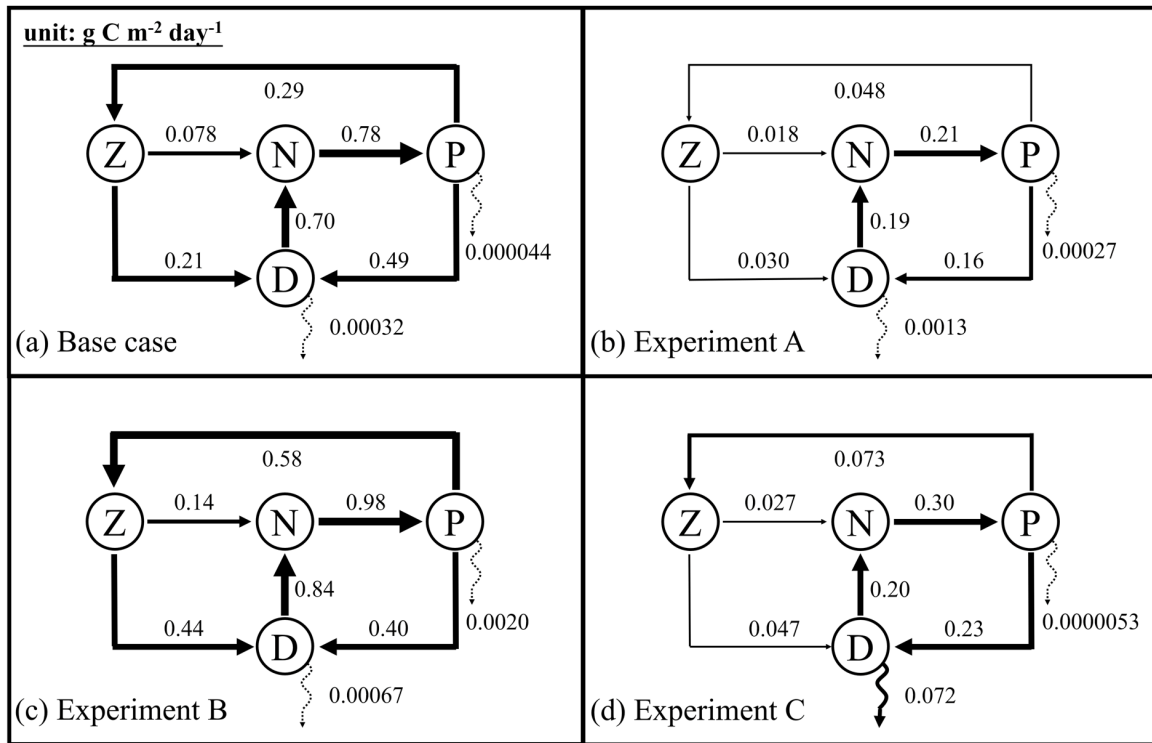
21

22

Figure 5. The case-specific cost function values (a-c) and total misfits (d) of the base case and the different

23

optimizations.



24

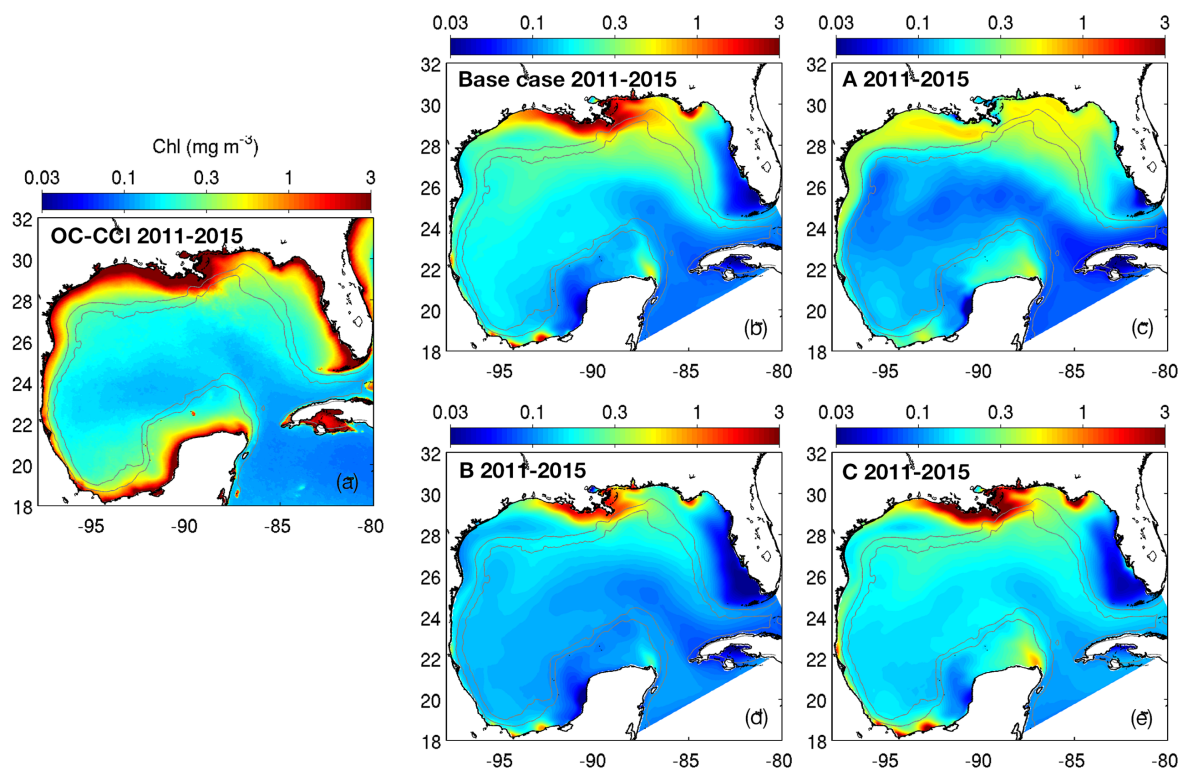
25 Figure 6. Annually averaged carbon fluxes integrated over the upper 200 m (unit: $\text{g C m}^{-2} \text{ day}^{-1}$) for the base case

26 (a) and optimized experiments A, B, and C. The N, P, Z, and D stand for the pools of nutrient, phytoplankton,

27 zooplankton, and the sum of small and large detritus, respectively. The thickness of arrows scales with the

28 magnitude of fluxes. Dashed arrows represent fluxes lower than $0.01 \text{ g C m}^{-2} \text{ day}^{-1}$.

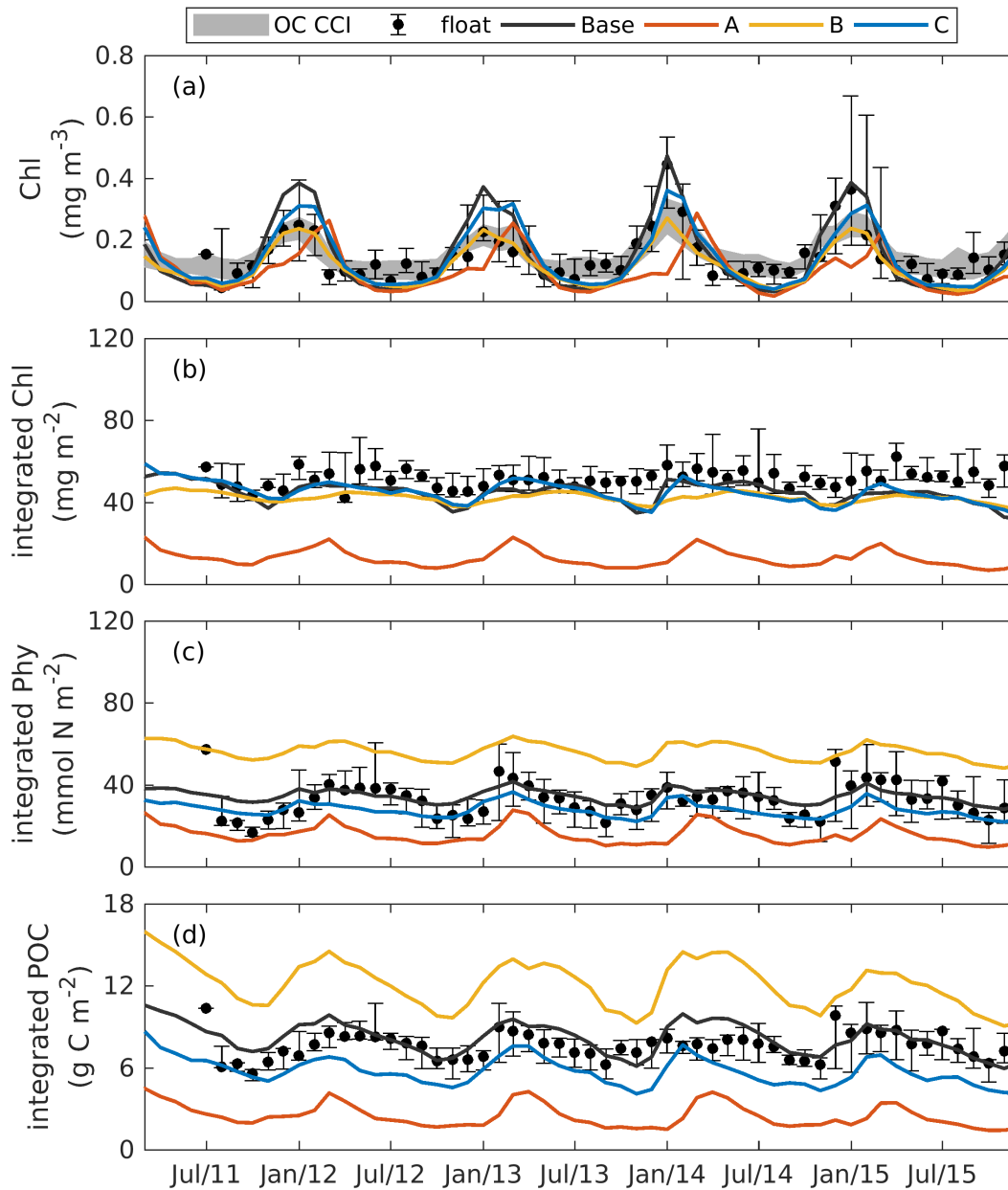
29



30

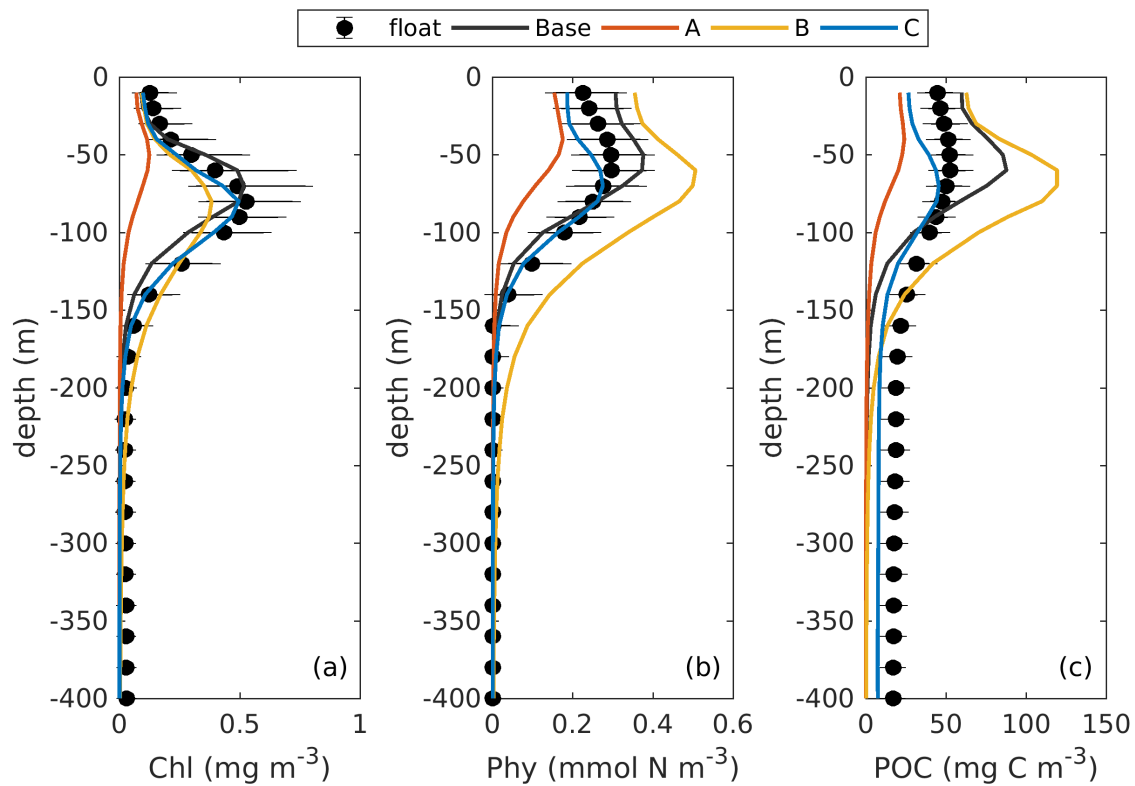
31 Figure 7. Spatial distributions of the annual mean chlorophyll in the surface layer from the satellite (OC-CCI)
 32 climatology (2011-2015) and the different model versions. The gray contours mark the bathymetric depths of 200
 33 and 1000 m.

34



35

36 Figure 8. Observed and simulated seasonal cycles of surface chlorophyll (a), vertically integrated chlorophyll (b),
 37 vertically integrated phytoplankton (c), and vertically integrated POC (d) from each 3D models. Solid lines
 38 represent the median values over the deep ocean of GOM (depth>1000m). Error bars and shades show the 25%
 39 and 75% percentiles. Chlorophyll, phytoplankton, and POC are integrated over the top 200m.

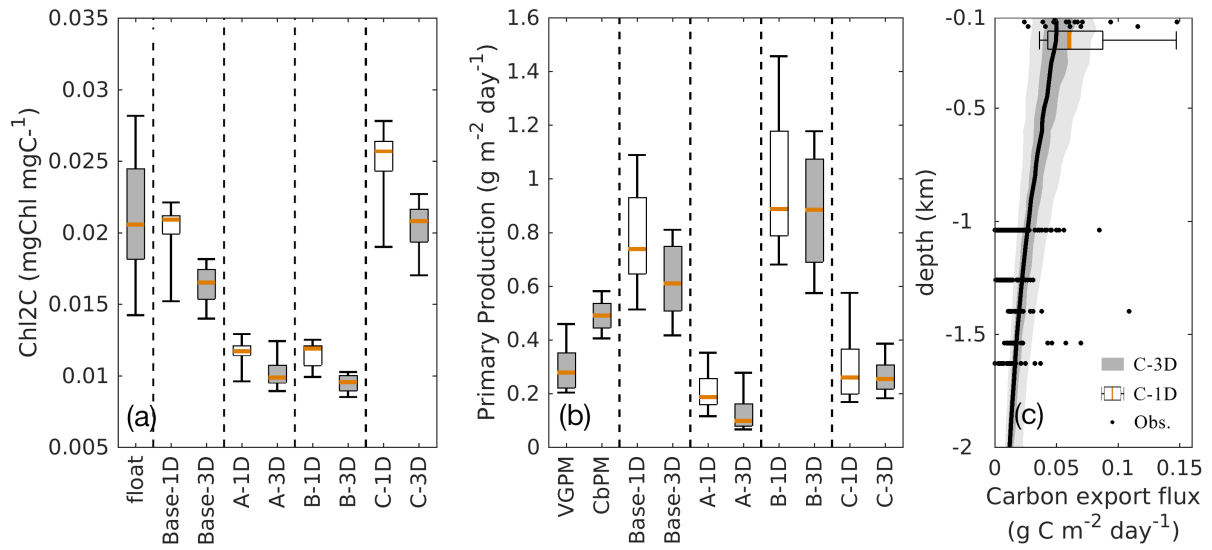


40

41 Figure 9. Observed and simulated vertical profiles of chlorophyll, phytoplankton, and POC from each 3D models.

42

43



44

45 Figure 10. Comparisons of the chlorophyll to carbon ratio (a), primary production (b), and carbon export fluxes (c)
 46 between the 1D and 3D models.

47

48